IAI Journals.ASM.org

Genetically Modified Live Attenuated *Leishmania donovani* Parasites Induce Innate Immunity through Classical Activation of Macrophages That Direct the Th1 Response in Mice

Parna Bhattacharya,[a] Ranadhir Dey,[a] Pradeep K. Dagur,[b] Michael Kruhlak,[c] Nevien Ismail,[a] Alain Debrabant,[a] Amritanshu B. Joshi,[a] Adovi Akue,[d] Mark Kukuruga,[d] Kazuyo Takeda,[d] Angamuthu Selvapandiyan,[e] John Philip McCoy, Jr.,[b] Hira L. Nakhasi[a]

Division of Emerging and Transfusion Transmitted Disease, Center for Biologics Evaluation and Research, Food and Drug Administration, Silver Spring, Maryland, USA[a]; Flow Cytometry Core, National Heart, Lung, and Blood Institute, National Institutes of Health, Bethesda, Maryland, USA[b]; Experimental Immunology Branch, National Cancer Institute, NIH, Bethesda, Maryland, USA[c]; Office of Vaccines Research and Review, Center for Biologics Evaluation and Research, Food and Drug Administration, Silver Spring, Maryland, USA[d]; Institute of Molecular Medicine, New Delhi, India[e]

Visceral leishmaniasis (VL) causes significant mortality and there is no effective vaccine. Previously, we have shown that genetically modified *Leishmania donovani* parasites, here described as live attenuated parasites, induce a host protective adaptive immune response in various animal models. In this study, we demonstrate an innate immune response upon infection with live attenuated parasites in macrophages from BALB/c mice both *in vitro* and *in vivo*. *In vitro* infection of macrophages with live attenuated parasites (compared to that with wild-type [WT] *L. donovani* parasites) induced significantly higher production of proinflammatory cytokines (tumor necrosis factor alpha [TNF-α], interleukin-12 [IL-12], gamma interferon [IFN-γ], and IL-6), chemokines (monocyte chemoattractant protein 1/CCL-2, macrophage inflammatory protein 1α/CCL-3, and IP-10), reactive oxygen species (ROS), and nitric oxide, while concomitantly reducing anti-inflammatory cytokine IL-10 and arginase-1 activities, suggesting a dominant classically activated/M1 macrophage response. The classically activated response in turn helps in presenting antigen to T cells, as observed with robust $CD4^+$ T cell activation *in vitro*. Similarly, parasitized splenic macrophages from live attenuated parasite-infected mice also demonstrated induction of an M1 macrophage phenotype, indicated by upregulation of IL-1β, TNF-α, IL-12, and inducible nitric oxide synthase 2 and downregulation of genes associated with the M2 phenotype, i.e., the IL-10, YM1, Arg-1, and MRC-1 genes, compared to WT *L. donovani*-infected mice. Furthermore, an *ex vivo* antigen presentation assay showed macrophages from live attenuated parasite-infected mice induced higher IFN-γ and IL-2 but significantly less IL-10 production by ovalbumin-specific $CD4^+$ T cells, resulting in proliferation of Th1 cells. These data suggest that infection with live attenuated parasites promotes a state of classical activation (M1 dominant) in macrophages that leads to the generation of protective Th1 responses in BALB/c mice.

The protozoan parasite *Leishmania donovani* is one of the major causative agents of visceral leishmaniasis (VL), which is the second most challenging infectious disease worldwide, with nearly 500,000 new cases and 60,000 deaths annually (1).

During their intracellular life cycle, *Leishmania* parasites survive as obligate pathogens that infect the hematopoietic cells of the macrophage/monocyte lineage, which they enter by phagocytosis (2) and establish infection within parasitophorous vacuoles (3). Macrophages, the major innate effector cells responsible for killing of *Leishmania* parasites (2), are markedly heterogeneous, displaying a combination of inflammatory and anti-inflammatory functions (4, 5). The two extremes in the spectrum of macrophage function are represented by classically activated (or M1) phenotype macrophages, which show leishmanicidal activity, and alternatively activated macrophages, which exhibit anti-inflammatory activity (the M2 phenotype) that favors parasite survival (4, 5).

Leishmania parasites have evolved intricate mechanisms to evade macrophage antimicrobial functions (6). *Leishmania*-induced macrophage dysfunctions have been correlated mainly with depletion of microbicidal molecules (6–8) and altered signaling events, which result in skewing of T helper (Th) cells to the disease-promoting anti-inflammatory Th2 subset (9). Importantly, the enhanced Th2 response during *Leishmania* infection leads to enhanced arginase activities in infected macrophages (10, 11), which subsequently suppress NO production and enhance polyamine production to facilitate parasite survival (10, 12). Furthermore, the high level of Th2 cytokine induction during *Leishmania* infection also mediates alternative activation (10, 11, 13), thereby suppressing the killing capacities of the macrophages (4). Specifically, interleukin-10 (IL-10), induced during *Leishmania* infection, inhibits the microbicidal activity of macrophages by attenuating the generation of nitric oxide (NO) and proinflammatory cytokines (4, 14). In addition, *Leishmania* infection displaces cho-

Received 11 February 2015 **Returned for modification** 9 April 2015
Accepted 7 July 2015

Accepted manuscript posted online 13 July 2015

Citation Bhattacharya P, Dey R, Dagur PK, Kruhlak M, Ismail N, Debrabant A, Joshi AB, Akue A, Kukuruga M, Takeda K, Selvapandiyan A, McCoy JP, Jr, Nakhasi HL. 2015. Genetically modified live attenuated *Leishmania donovani* parasites induce innate immunity through classical activation of macrophages that direct the Th1 response in mice. Infect Immun 83:3800–3815. doi:10.1128/IAI.00184-15.

Editor: J. H. Adams

Address correspondence to Hira L. Nakhasi, Hira.Nakhasi@fda.hhs.gov.

Supplemental material for this article may be found at http://dx.doi.org/10.1128/IAI.00184-15.

doi:10.1128/IAI.00184-15

lesterol from the macrophage membrane, leading to enhanced membrane fluidity and inhibiting its ability to display parasite antigens to other cells of the immune system (15, 16). Together, this complex process enables the parasite to evade the innate immune response and replicate within the phagolysosomal compartments of the infected macrophage.

In contrast to alternative activation, classical activation of macrophages (CAM) is characterized by the induction of antimicrobial mediators such as NO and reactive oxygen species (ROS), which are critical for parasite clearance (7, 8, 17, 18). Additionally, CAM entails secretion of a battery of inflammatory cytokines, such as tumor necrosis factor alpha (TNF-α), IL-1β, and IL-12, which help to orchestrate and amplify Th1 immune responses (19–22). Specifically, IL-12 is a critical cytokine required for $CD4^+$ Th1 development and production of gamma interferon (IFN-γ), thereby providing a link between the innate response and the development of the antigen-specific adaptive immune response (4, 23). The outcome of infection in leishmaniasis is mainly determined by the balance between host protective Th1 (or proinflammatory) versus disease-promoting Th2 (or anti-inflammatory) effector responses, and in this context the production of IL-12 and IL-10 (24) by the classical/M1 and alternative/M2 macrophages, respectively, is important for this decision (4, 5, 22). Thus, macrophages play a crucial role in protection against *Leishmania* infection. It is worth mentioning here that the effective clearance of parasites by macrophages also depends on activation of an appropriate immune response, which is usually initiated by dendritic cells (DCs) (4). Indeed, several reports have shown a central role for DCs in orchestrating immune responses in leishmaniasis by controlling the induction of the protective Th1 response against *Leishmania* (25, 26).

Apart from dendritic cells, classical/proinflammatory/M1 macrophages also participate in the induction of a polarized Th1 response and have been associated with resistance to intracellular pathogens (22, 27–31). Of interest, such a polarization of T cells by proinflammatory (M1) macrophages was associated with induction of protection in several vaccine studies, including studies of recombinant *Mycobacterium bovis* BCG, attenuated West Nile virus (WNV), and live attenuated measles virus (32–34). These studies have shown that the aforementioned vaccine candidates manipulate the macrophages to enhance proinflammatory responses and yield improved protection against tuberculosis or WNV or measles virus infection.

Our laboratory has developed two *L. donovani* mutant cell lines, i.e., $Ldp27^{-/-}$ (with deletion of the *Ldp27* gene) (35) and $LdCen^{-/-}$ (with deletion of the *Centrin1* gene) (36) lines. The amastigote-stage-specific *Ldp27* gene is an essential component of the cytochrome *c* oxidase complex and is involved in oxidative phosphorylation, whereas *Centrin1* is a growth-regulating gene involved in cell division in the protozoan parasite *Leishmania*. Of note, both $Ldp27^{-/-}$ and $LdCen^{-/-}$ cells are specifically attenuated at the amastigote stage, suggesting that they have reduced virulence and could be used as live attenuated vaccine candidates. Indeed, the limited efficacies of vaccines based on DNA, subunits, or heat-killed parasites have led to the conclusion that attainment of durable immunity against the protozoan parasites requires a controlled infection with a live attenuated organism (37, 38). The live attenuated vaccines allow the host immune system to interact with a broad repertoire of antigens considered crucial in the development of protective immunity and, notably, cause no pathology (39). Recently, we demonstrated that these genetically modified *L. donovani* parasites ($Ldp27^{-/-}$ and $LdCen^{-/-}$) when used as vaccine candidates induced protection against virulent *L. donovani* infection in various animal models (mice, hamsters, and dogs), as indicated by control of parasitemia and the induction of a host protective T cell response (40–43). Since macrophage activation plays an important role in the commitment of T cells to either a protective (Th1) or disease-causing (Th2) phenotype during *Leishmania* infection (44), it is essential to study the role of macrophages and their phenotypes (M1 and M2) in live attenuated parasite-induced immunity.

Hence, in the present study we have investigated the early innate immune responses to these live attenuated parasites in mouse macrophages and compared them to those induced by WT *L. donovani* parasites both *in vitro* and *in vivo*. We found that infection with live attenuated parasites significantly enhanced the production of a proinflammatory response in bone marrow-derived macrophages (BMDM) compared to that induced by WT *L. donovani* parasite infection *in vitro*, thereby indicating classical activation of macrophages. Interestingly, $Ldp27^{-/-}$ cells complemented with the *Ldp27* gene (added back [AB]; $Ldp27^{-/-}$AB) and $LdCen^{-/-}$ cells complemented with the *Centrin1* gene ($LdCen^{-/-}$AB) behaved like WT *L. donovani* parasites and subsequently generate an anti-inflammatory immune response in macrophages. Further, live attenuated parasite-infected macrophages were able to promote the proliferation of $CD4^+$ T cells and induced strong Th1-type immune responses *in vitro*. Similarly, *in vivo* studies showed that parasitized splenic macrophages isolated from live attenuated parasite-infected BALB/c mice after 7 days of infection displayed upregulation of many classical activation or M1 macrophage markers, along with downmodulation of several alternative activation or M2 macrophage markers, compared to WT-infected mice. Further, in live attenuated parasite-infected mice, the antigen-presenting abilities of macrophages were skewed toward a more effective Th1 response. These studies confirmed that the protective adaptive immune response generated by live attenuated parasites against wild-type *L. donovani* challenge previously observed by us (40–43) is directed by the innate response generated by host macrophages.

MATERIALS AND METHODS

Animals and parasites. Five- to 6-week-old female BALB/c mice from the National Cancer Institute were used in the experiments. Five- to 6-week-old ovalbumin (OVA) peptide-specific H-2^d (IA^d-restricted) T cell receptor transgenic DO11.10 mice (BALB/c background) obtained from the Jackson Laboratory were used for the antigen presentation experiment. Procedures used were reviewed and approved by the Animal Care and Use Committee, Center for Biologics Evaluation and Research, Food and Drug Administration. Among parasites, the WT, p27 gene-deleted ($Ldp27^{-/-}$), *Ldp27* episomal add-back ($Ldp27^{-/-}$AB), *Centrin1* gene-deleted ($LdCen^{-/-}$), and *LdCen* episomal add-back ($LdCen^{-/-}$AB) lines of *L. donovani* were used. The parasite culture procedure and the routine molecular biology practices were as previously described (35, 40). Red fluorescent protein (RFP)-expressing WT *L. donovani* and $Ldp27^{-/-}$ parasites were developed using the pA2RFPhyg plasmid for the integration of an RFP/hygromycin B resistance gene expression cassette into the parasite's 18S rRNA gene locus, as described previously (45). mCherry-expressing $LdCen^{-/-}$ parasites were generated using the pLEXSY-mCherry-sat2 plasmid, following the manufacturer's protocol (Jena Bioscience). The parasites were cultured according to a procedure previously described (46).

Preparation of bone marrow-derived macrophages, *in vitro* infection, and stimulation. Bone marrow cells were isolated from the femurs and tibias of BALB/c mice (47). Briefly, after depletion of erythrocytes with ACK (ammonium-chloride-potassium) lysis buffer (Lonza), the cells were seeded in cell culture dishes and cultured with complete RPMI medium supplemented with 10% (vol/vol) fetal bovine serum, 1% penicillin, 20 units/ml streptomycin, and 20 ng/ml macrophage colony-stimulating factor at 37°C in a CO_2 incubator for differentiation into macrophages. The cells were washed twice with phosphate-buffered saline (PBS) every 2 to 3 days, and fresh medium was added. Macrophage progenitor cells adhere to the cell dish and are not washed away, whereas nonadherent dead cells are washed away. Macrophages are fully differentiated at day 6. On day 7, the cells were washed thrice with PBS, the differentiated adherent live macrophage population was detached from the plate with a solution containing trypsin (Life Technologies), and cells were processed for phenotypic characterization. Based on the specific expression of the number of surface markers, including CD11b, CD14, and F4/80 (BD Pharmingen), along with analysis using the Live/Dead Fixable Aqua system (Invitrogen/Molecular Probes), >90% pure live macrophages were obtained as evaluated by flow cytometry.

For *in vitro* infection, stationary-phase cultures of WT, live attenuated parasites (*Ldp27*$^{-/-}$, *LdCen*$^{-/-}$), and gene-complemented add-back parasites (*Ldp27*$^{-/-}$AB, *LdCen*$^{-/-}$AB) promastigotes were incubated in 10% mouse (BALB/c) serum for 15 min at 37°C for complement opsonization, followed by washing with PBS three times. Thereafter, BMDM were incubated with these opsonized parasites (5:1, parasite/macrophage ratio) and, after 6 h, cells were washed with culture medium to remove the extracellular parasites. Then, infected cells were cultured at 37°C for different lengths of time. In some experiments, infected BMDM were treated with or without lipopolysaccharide (LPS; Sigma) at 1 μg/ml or recombinant IFN-γ (rIFN-γ; 100 U/ml; Sigma) for 24 h.

Phagocytosis and parasite clearance assay. BALB/c mouse BMDM were harvested and seeded into Lab-Tek culture chamber incubation slides (Nunc, Naperville, IL) at 5×10^4 cells per chamber. Thereafter, for phagocytosis and parasite clearance assays, cells were infected with the opsonized WT *L. donovani*, live attenuated, or add-back stationary-phase promastigotes for 6 h at 37°C in 5% CO_2 and washed with the medium, and then the cultures were incubated in RPMI medium for a maximum of 72 h. At 6, 24, 48, and 72 h postinfection, the culture medium was removed from a sample of the culture slides, the slides were air dried, fixed by immersion in absolute methanol for 5 min at room temperature, and stained using a Diff-Quick stain set (Baxter Healthcare Corp., Miami, FL), and intracellular parasite numbers were evaluated microscopically. To measure parasite load in these cultures, a minimum of 300 macrophages were counted. The results are expressed either as percentages of macrophages that were infected by parasites or as the mean number of parasites/infected macrophage.

Measurement of ROS. For monitoring the level of ROS (including superoxide, hydrogen peroxide, and other reactive oxygen intermediates) produced within the cell, the cell-permeable, nonpolar, H_2O_2-sensitive probe dichlorofluorescein diacetate (DCFDA) was used (48). Briefly, mouse BMDM harvested at different infection time points were incubated with H_2DCFDA (2 μg/ml) at room temperature for 20 min in the dark. The extent of H_2O_2 generation was defined as the generated ROS, for our convenience. Relative fluorescence was measured in a Spectramax instrument (Molecular Diagnostics) at an excitation wavelength of 510 nm and an emission wavelength of 525 nm. For each experiment, fluorometric measurements were performed in triplicate, and data are expressed in mean fluorescence intensity units.

Quantification of nitric oxide. Nitrite accumulation in culture was measured colorimetrically via the Griess assay (41). For each assay, freshly generated BMDM were cultured in 96-well tissue culture plates at a concentration of 10^5 cells/ml followed by infection with different groups of opsonized parasites and then stimulation with or without LPS (1 μg/ml) or rIFN-γ (100 U/ml) for 24 h. Cell-free supernatants were collected at 24 h postinfection from different experimental sets, and nitrite levels were estimated in accordance with the manufacturer's instructions. When indicated, the nitrite generation was measured in the presence and absence of the p38 mitogen-activated kinase (MAPK) inhibitor SB203580 (10 μg/ml; Sigma).

Arginase activity assay. Arginase activity (reported in international units), measuring based on the conversion of arginine to ornithine and urea, was determined with a quantitative colorimetric assay at 430 nm and by employing an arginase assay kit (Bioassay Systems) according to the kit instructions.

Preparation of cell lysates and immunoblot analysis. Cell lysates were prepared as described elsewhere (49). Equal amounts of protein (50 μg) were subjected to 10% sodium dodecyl sulfate-polyacrylamide gel electrophoresis, and immunoblotting was performed to detect the expression of iNOS2, arginase-1, and phosphorylated forms of p38 MAPK. Using the same lysate, a separate immunoblotting assay was performed to detect the β-actin and dephosphorylated form of p38 MAPK.

Confocal microscopy. For fluorescence confocal microscopy, BMDM were grown on coverslip chambered slides, infected with various groups of opsonized parasites and stimulated with LPS (1 μg/ml; Sigma) for 24 h. Cells were then washed, fixed (3% [vol/vol] paraformaldehyde), permeabilized, blocked (10% goat serum, 5% glycerol, 0.1% Nonidet P-40 in PBS), and then stained with fluorescein isothiocyanate (FITC)-conjugated LAMP-1 antibody (green stain) and phycoerythrin (PE)-conjugated iNOS2 antibody (red stain) for 30 min. After the immunolabeling reaction, the preparation was washed thoroughly with PBS, and nucleic acids were stained with 4′,6-diamidino-2-phenylindole, which stains both the cell nucleus and parasite DNA (blue stain). The cells were then examined for fluorescence with an LSM510 Meta Zeiss confocal microscope (Carl Zeiss Microscopy, LLC, Thornwood, NY).

For filipin staining, BMDM were infected with various groups of fluorescent parasites (red fluorescent WT RFP, *Ldp27*$^{-/-}$ RFP, or *LdCen*$^{-/-}$ mCherry), and paraformaldehyde-fixed cells were incubated for 30 min with filipin (0.5 mg/ml in PBS; Sigma) and then washed with PBS. Cells stained with filipin were imaged using the 364-nm UV laser on the Zeiss LSM510 Meta microscope, with fluorescence emission collected using a 435- to-485-nm band-pass emission filter.

Flow cytometry. BMDM were infected with various groups of opsonized parasites for 24 h. The cultures were then collected, fixed for 30 min with 3% (vol/vol) paraformaldehyde in PBS at room temperature, stained with 50 μg/ml filipin (Sigma) in PBS, and analyzed by flow cytometry. For surface staining, cells were blocked at 4°C with rat anti-mouse CD16/32 (5 mg/ml; BD Pharmingen) for 20 min. Cells were then stained with anti-mouse CD40–FITC conjugate, anti-mouse CD80–PE conjugate, anti-mouse CD86–allophycocyanin, and anti-mouse major histocompatibility complex class II (MHC-II)–Alexa Fluor 700 (eBioscience) conjugate for 30 min (each at a 1:200 dilution) at 4°C. The cells were then stained with the Live/Dead Fixable Aqua system (Invitrogen/Molecular Probes), which stains dead cells. Cells were washed with wash buffer and were finally suspended in PBS plus 1% paraformaldehyde and were kept at 4°C in the dark until acquired for cytometry analysis. Cells were acquired on a Fortessa apparatus (BD Biosciences, USA) equipped with 355-, 405-, 488-, 532-, and 638-nm laser lines and FACSDIVA 8.0 software (BD). Data were analyzed with the FlowJo software version 9.7.5.

Multiplex cytokine enzyme-linked immunosorbent assay (ELISA). BMDM were plated in 96-well plates, infected with different groups of opsonized parasites, and treated with LPS for 24 h. Culture supernatants were then analyzed using the Multiplex mouse cytokine/chemokine magnetic panel (Millipore, USA) and a Luminex-100 system (Luminex, Austin, TX, USA) with Bioplex Manager software version 5.0, according to the manufacturer's instructions. When indicated, cytokine generation was measured in the presence and absence of the p38 MAPK inhibitor SB203580 (10 μg/ml; Sigma).

Cytokine ELISA. The conditioned media of macrophage cultures after infection with WT, live attenuated, and add-back *L. donovani* parasites

were assayed for mouse cytokines via sandwich ELISA kit (eBioscience). The assay was performed according to the manufacturer's instructions.

Antigen presentation assay. (i) *In vitro* BMDM and T cell coculture studies. BMDM were pulsed with an OVA peptide (2 μg/ml; residues 323 to 339; Anaspec) and infected with WT or live attenuated parasites for 24 h. $CD4^+$ T cells were purified from spleens of DO11.10 transgenic mice (mice carrying this MHC class II-restricted, rearranged T cell receptor transgene on an H-2^d background react to the ovalbumin peptide antigen) stained with 5 μM carboxyfluorescein succinimidyl ester (CFSE; Molecular Probes/Invitrogen) for 10 min in RPMI 1640 without fetal calf serum (FCS) at 37°C in a 5% CO_2 humidified chamber. After this, cells were incubated for 5 min with ice-cold RPMI 1640 plus 10% FCS for quenching the CFSE and subsequently washed thoroughly before plating in 96-well tissue culture plates along with OVA-pulsed BMDM. Cells were cultured for 5 days at 37°C with 5% CO_2, and T cell proliferation was then estimated by flow cytometry by gating on $CD4^+$ cells. For each sample, 10,000 CD4-positive cells were measured. FlowJo software version 9.7.5 was used. Culture supernatants were collected at day 5 to evaluate cytokines via an ELISA using a sandwich ELISA kit (eBioscience). The assay was performed as per the detailed instructions of the manufacturer.

In a separate experiment, the T cell proliferation capacity of the OVA-pulsed, infected BMDM and T cell coculture experiment was measured as described above. Briefly, cocultures were incubated for 5 days, stained with anti-CD4–FITC and fixed, and then intracellular staining was performed with Ki67-PE to determine proliferation via flow cytometry as described above.

(ii) *Ex vivo* BMDM and T cell coculture studies. BMDM isolated from different groups of infected mice (either WT or live attenuated parasites) were pulsed with OVA peptide followed by an *in vitro* coculture experiment with OVA-specific $CD4^+$ T cells isolated and purified from DO11.10 transgenic mice and labeled with CFSE. After 5 days of incubation at 37°C in a 5% CO_2, humidified chamber, T cell proliferation was measured by studying the dilution of CFSE in anti-CD4-stained T cells via flow cytometry. CFSE low gating showed the frequencies of proliferating $CD4^+$ T cells in response to coculture with infected BMDM with different leishmanial cell lines. The cytokine production was assessed in the coculture supernatants by using a sandwich ELISA kit (eBioscience).

Measurement of FA. The membrane fluorescence and lipid fluidity of cells were measured as described elsewhere (15). Briefly, the fluorescent probe 1,6-diphenyl-1,3,5-hexatriene (DPH) was dissolved in tetrahydrofuran at 2 mM and then added to 10 ml of rapidly stirring PBS (pH 7.2). The cells were labeled by mixing 10^6 cells with an equal volume of DPH in PBS (concentration factor, 1 μM) and incubated for 2 h at 37°C. The cells were then washed three times and resuspended in PBS. The DPH probe bound to the membranes of the cells was excited at 365 nm, and the intensity of emission was recorded at 430 nm in a spectrofluorometer. The fluorescence anisotropy (FA) value was calculated using the following equation: $FA = (I_{\parallel} - I_{\perp})/(I_{\parallel} + 2I_{\perp})$, where $I_{\parallel}$ and $I_{\perp}$ are the fluorescence intensities oriented, respectively, parallel and perpendicular to the direction of polarization of the excited light.

Infection of mice, parasite burden estimation, and parasitized splenic macrophage isolation. Mice were infected via tail vein with 3×10^6 stationary-phase RFP-labeled WT, *Ldp27*$^{-/-}$, or *LdCen*$^{-/-}$-mCherry promastigotes. In each study, at least 6 mice were used per group. Age-matched naive mice were used as controls. At 7 day postinfection, mice were sacrificed and the parasite load was recorded from spleens of the WT *L. donovani*-infected and live attenuated parasite-infected mice by culturing the separated host cell preparations by limiting dilution as previously described (40, 41).

In a separate experiment, the splenic macrophages were sorted (50). Single-cell suspensions were prepared from spleens, and red blood cells (RBCs) were lysed using ACK lysing buffer. Sorting of *Leishmania* (RFP-mCherry)-infected splenic macrophages (IM) and uninfected splenic macrophages (UIM) from different groups of mice was performed using a high-speed fluorescence-activated cell sorter (FACS) system (FACS AriaIITM; BD). Infected splenic macrophages were sorted by gating live single cell lineage$^-$ (T cell, B cell, NK cell) RFP-mCherry$^+$ cells. Next, lineage$^-$ mCherry$^+$ cells were gated for MHC-II$^+$ CD11b$^+$ myeloid cells, which were then gated for the Cd11c$^-$ Ly6G$^-$ population. Uninfected splenic macrophages (lineage$^-$ [T cell, B cell, NK cell] RFP-mCherry$^-$ Cd11b$^+$ MHC-II$^+$ Cd11c$^-$ Ly6G$^-$) were also sorted.

RT-PCR. Total RNA was extracted from the parasitized and uninfected splenic macrophages by using an RNAqueous microkit (AM1931; Ambion). Aliquots (400 ng) of total RNA were reverse transcribed into cDNA by using random hexamers from a high-capacity cDNA reverse transcription (RT) kit (Applied Biosytems). Gene expression levels were determined using the TaqMan gene expression master mix and premade TaqMan gene expression assays (Applied Biosystems) and a CFX96 Touch real-time system (Bio-Rad, Hercules, CA). The data were analyzed with CFX Manager software. The TaqMan gene expression assay primers (Applied Biosystems) used were as follows: iNOS2, Mm00440502_m1; IL-1β, Mm00434228_m1; TNF-α, Mm00443258_m1; IL-12, Mm00434174_m1; arginase-1, Mm00475988_m1; MRC-1, Mm00485148_m1; YM1, Mm00657889_m1; IL-10, Mm00439614_m1; glyceraldehyde-3-phosphate dehydrogenase (GAPDH), Mm99999915_m1. Expression values were determined by the cycle threshold ($2^{-\Delta\Delta CT}$) method, and results were normalized to GAPDH expression levels and reported relative to results with the untreated sample.

Statistical analysis. Statistical analysis of differences between means of groups was determined via an unpaired two-tailed Student *t* test, using GraphPad Prism 5.0 software. A *P* value of <0.05 was considered significant, and a *P* value of <0.005 was considered highly significant.

RESULTS

Evaluation of WT and live attenuated parasite infection in BMDM *in vitro*. We have previously shown that live attenuated parasites, which are phagocytized by human macrophages, have reduced survival compared to WT parasites (35, 36). In this study, we investigated the rates of phagocytosis and infectivity of live attenuated parasites in mouse BMDM. *In vitro*-differentiated BMDM were inoculated with stationary-phase cultures of WT, live attenuated (*Ldp27*$^{-/-}$, *LdCen*$^{-/-}$), or add-back (*Ldp27*$^{-/-}$AB, *LdCen*$^{-/-}$AB) promastigotes. At 6 h postinfection, there were no significant differences in the percentage of infected cells or in the number of parasites per infected cell between WT, live attenuated, or add-back parasite-infected cells (Fig. 1A and B). These BMDM cultures were then subsequently examined at 24, 48, and 72 h postinfection, and the percentages of infected macrophages and parasite load were calculated. Interestingly, BMDM infected with live attenuated parasites displayed a significantly lower percentage of infected cells (Fig. 1A) and fewer parasites per infected cell (Fig. 1B) than BMDM infected with WT or add-back parasites at all time points postinfection. Thus, live attenuated parasites (*Ldp27*$^{-/-}$, *LdCen*$^{-/-}$) are capable of infecting macrophages at rates similar to the WT but are unable to persist in BMDM for prolonged periods compared to WT parasites, and this is a direct consequence of the deficiency of *Ldp27* and *Centrin1* genes, respectively, as demonstrated by adding back the corresponding gene in the parasites.

Live attenuated parasites induced a strong effector function in BMDM, thereby promoting classical activation *in vitro*. Classical activation of macrophages is characterized by the induction of ROS and NO (17, 19), which have been identified as critical oxidative agents in controlling *Leishmania* infection (6–8). We studied the generation of these two molecules in response to live attenuated parasite infection. BMDM were incubated for 15, 30, 60, 120, and 240 min with WT or live attenuated parasite promas-

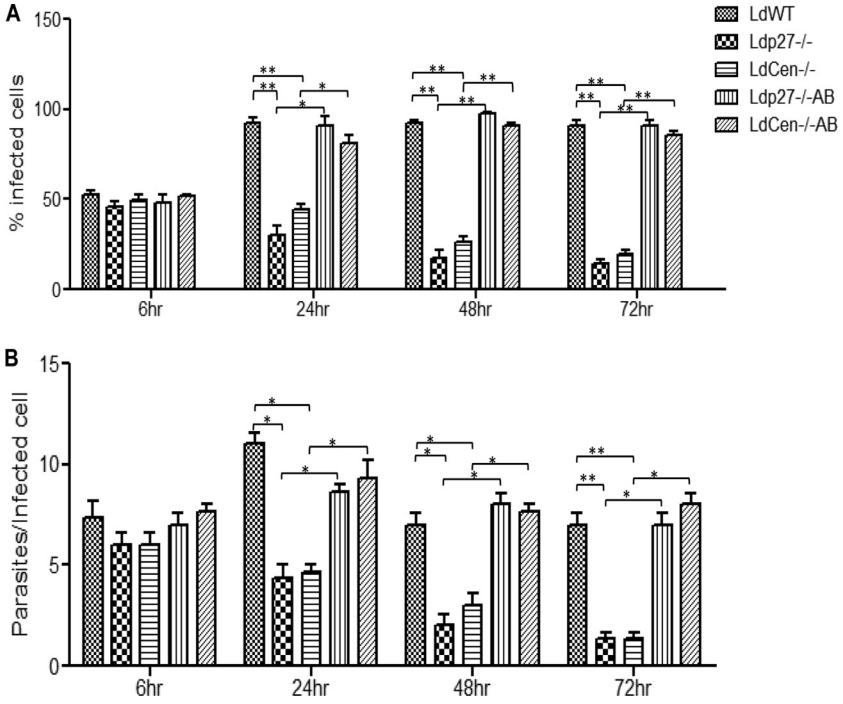

FIG 1 Phagocytosis rate and infectivity of WT and live attenuated parasites in BMDM. BMDM were infected with opsonized WT *L. donovani* parasites, live attenuated parasites ($Ldp27^{-/-}$ or $LdCen^{-/-}$) or gene-complemented add-back parasites ($Ldp27^{-/-}$AB, $LdCen^{-/-}$AB) (5:1, parasite to macrophage ratio). Intracellular parasite numbers were visualized by Giemsa staining and estimated microscopically at 6 h, 24 h, 48 h, and 72 h postinfection. (A and B) The infection efficiency (percentage of infected cells) (A) and intracellular growth (parasites per infected cell) (B) were recorded. To measure parasite load in these cultures, a minimum of 300 macrophages were counted. The data represent the means ± standard deviations of three independent experiments that all yielded similar results. *, $P < 0.05$; **, $P < 0.005$.

tigotes, and ROS levels were assayed. We observed that WT parasites induced ROS production only at 30 min postinfection, compared to uninfected BMDM (Fig. 2A, arrow). However, live attenuated parasite infection induced ROS generation in a sustained manner starting from 30 min up to 120 min postinfection compared to WT-infected BMDM (Fig. 2A).

Next, we analyzed the level of NO, a prototypic classical activation marker in mouse macrophages (20), in BMDM cell supernatants 24 h postinfection upon simulation with either LPS or rIFN-γ. Interestingly, live attenuated parasite-infected BMDM secreted significantly more NO than WT-infected cells in response to LPS or rIFN-γ (Fig. 2B). Because the generation of NO is dependent on the activation of iNOS2, we studied iNOS2 expression at the protein level. A significant increase in iNOS2 expression was observed in live attenuated parasite-infected BMDM compared to the WT-infected BMDM stimulated with LPS (Fig. 2C) or rIFN-γ (Fig. 2D). Of note, without LPS or rIFN-γ stimulation, NO production was observed at nonsignificant levels in uninfected macrophages (Fig. 2B, C and D) and in infected macrophages (data not shown). Moreover, to examine whether iNOS2 induced by live attenuated parasites was in the parasitophorous vacuole, so that NO produced was in the right place to control parasitemia, we performed confocal analysis using a fluorescence-labeled anti-LAMP antibody, a marker for the parasitophorous vacuole, and an anti-iNOS2 antibody in parasitized BMDM 24 h postinfection. Imaging by confocal microscopy revealed that the enhanced iNOS2 was mostly localized in the vicinity of parasitophorous vacuoles of live attenuated parasite-infected BMDM (Fig. 2E). Altogether, these observations suggest that BMDM infected with live attenuated parasites undergo a more pronounced oxidative burst in response to either LPS or rIFN-γ than do WT-infected macrophages.

Additionally, the anti-inflammatory/Th2 cytokine induced enhanced arginase-1 expression in host cells during *Leishmania* infection and impaired NO production, leading to parasite survival and alternative macrophage activation (4, 10–13). Hence, we sought to determine the arginase-1 activity in live attenuated parasite-infected BMDM. We found enhanced arginase-1 activity and expression in WT-infected BMDM at 24 h postinfection in response to either LPS or rIFN-γ stimulation (Fig. 2F, G, and H). In contrast, live attenuated parasite-infected BMDM showed substantially reduced activity and expression of arginase-1 in response to the stimulation (Fig. 2F, G, and H). However, it has been suggested that *Leishmania* parasites express endogenous arginase-1 (11, 13). Hence, we measured endogenous arginase-1 expression in purified amastigotes of WT and live attenuated parasites to assess the contribution of *Leishmania* arginase-1 to total arginase-1 activity. In our studies, we did not detect arginase-1 protein by Western blotting in purified amastigotes (data not shown). This observation indicated that arginase-1 expression from amastigotes did not contribute to arginase-1 expression measured in the BMDM. Collectively, these results suggest that the higher rates of live attenuated parasite clearance might be the result of enhanced ROS, NO generation, and attenuated arginase-1 activity, thereby promoting classical activation of BMDM *in vitro*.

***In vitro* modulation of pro- and anti-inflammatory cytokine and chemokine responses by WT-infected and live attenuated parasite-infected BMDM.** We evaluated the cytokine response in culture supernatants of uninfected and infected BMDM to exam-

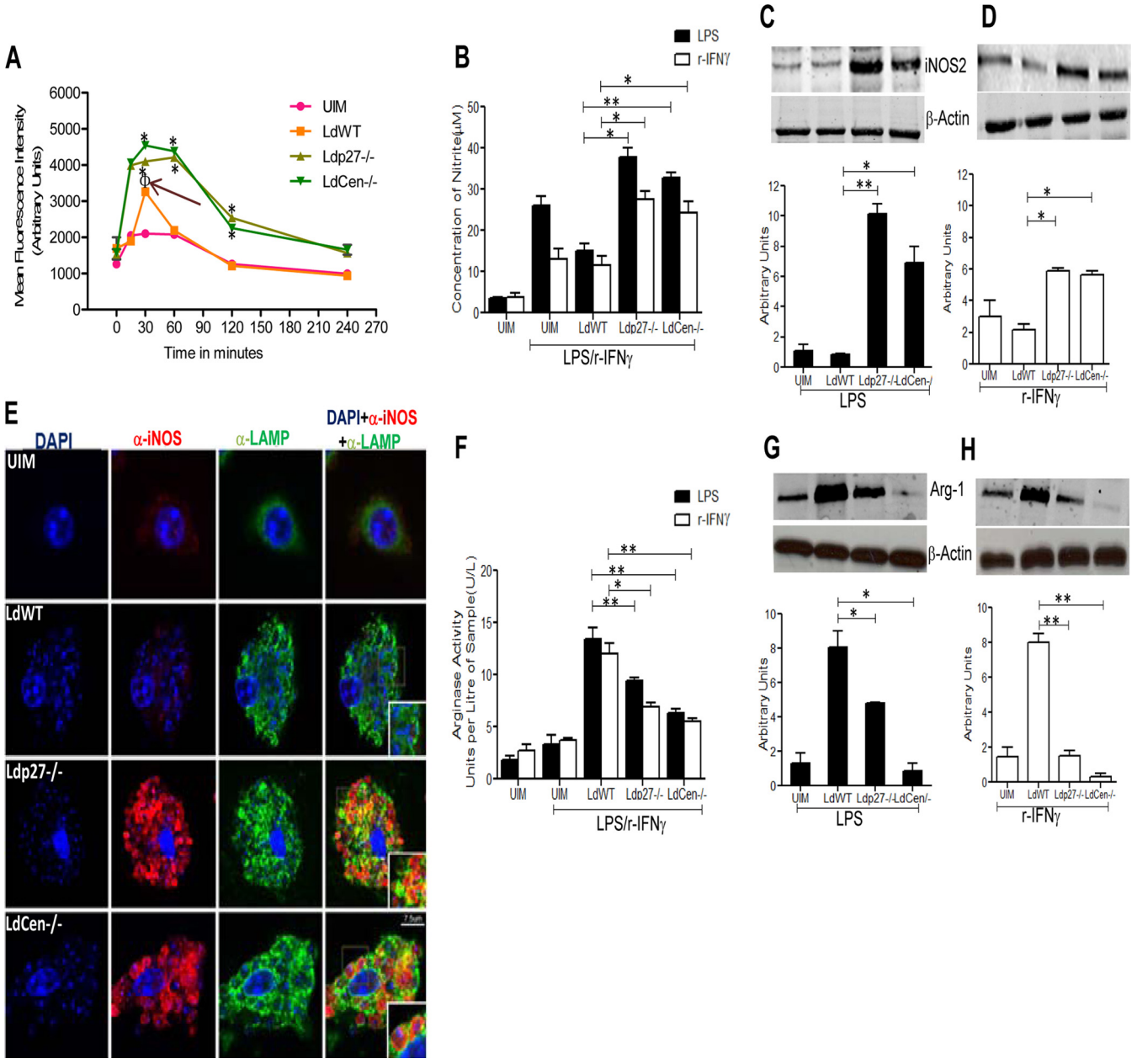

FIG 2 Live attenuated parasite infection generates effectors (ROS and NO) along with the attenuation of arginase-1 activity in BMDM in response to LPS or rIFN-γ stimulation, compared to WT infection *in vitro*. BMDM were either left uninfected or infected with various groups of opsonized parasites for the indicated time periods. (A) ROS generation was measured by H_2DCFDA staining of the BMDM. Data for ROS generation (MFI, in arbitrary units) are expressed as means ± standard deviations (SD) from triplicate experiments that yielded similar results. Φ, $P < 0.05$ compared to UIM; *, $P < 0.05$ compared to WT-infected BMDM. (B) In a separate experiment, BMDM were left uninfected or infected with different groups of parasites and treated with LPS (1 μg/ml) or rIFN-γ (100 U/ml) for 24 h. Cell-free supernatants were then collected to analyze NO production in the Griess assay as described in Materials and Methods. The data presented are the means ± SD of 3 independent experiments. *, $P < 0.05$; **, $P < 0.005$ compared to WT-infected BMDM. (C and D) The nature of iNOS2 expression was determined by Western blotting of BMDM cell lysates uninfected or infected with parasites and treated with LPS or rIFN-γ for 24 h as described above. The blot shown is a representative of experiments performed in triplicate. Band intensities were analyzed by densitometry and are represented by the bar diagram below each blot. The data presented are means ± SD of 3 independent experiments. *, $P < 0.05$; **, $P < 0.005$ compared to WT-infected BMDM. (E) BMDM were either left uninfected or infected with various groups of parasites and stimulated with LPS for 24 h as described above. The cells were then processed for immunofluorescence microscopy as described in Materials and Methods. α, antibody. Cells were observed under a confocal laser-scanning microscope. Optical sections (0.3 to 0.5 μm thickness) are shown. The micrographs are representative of 3 independent experiments in which at least 100 cells per sample were analyzed. Bar, 7.5 μm. (F to H) BMDM were either left uninfected or infected with various groups of opsonized parasites and then stimulated with LPS or rIFN-γ for 24 h as described above. From the cell lysates, arginase-1 activity was detected by using an arginase activity assay kit (F), and arginase-1 expression was measured in a Western blot assay (G and H) as described in Materials and Methods. The results are representative of 3 independent experiments with similar findings. Band intensities were analyzed by densitometry and are represented by the bar diagram below each blot. *, $P < 0.05$; **, $P < 0.005$ compared to WT-infected BMDM.

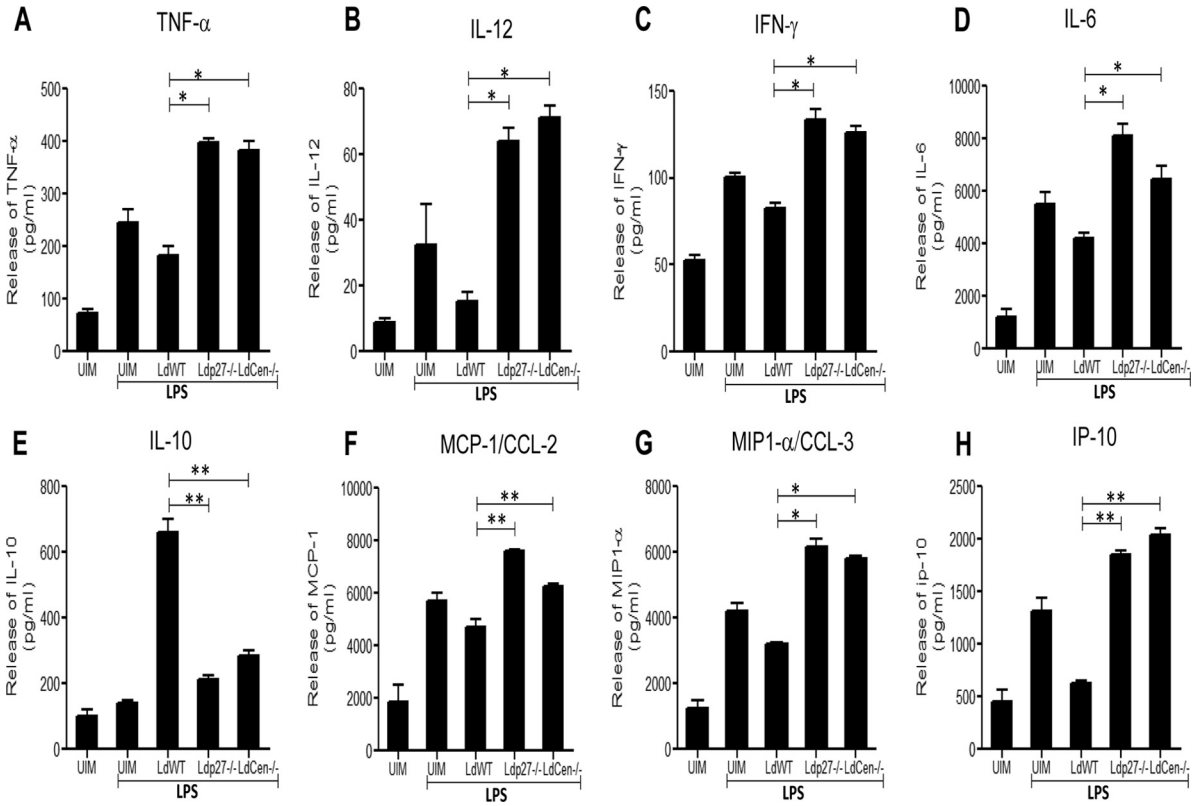

FIG 3 Live attenuated parasite infection induces proinflammatory cytokine and chemokine production and dampens anti-inflammatory cytokine generation in BMDM *in vitro*. BMDM were either left uninfected or infected with various groups of parasites and stimulated with LPS for 24 h as described in the legend for Fig. 2. After 24 h, the levels of TNF-α (A), IL-12 (B), IFN-γ (C), IL-6 (D), IL-10 (E), MCP-1/CCL-2 (F), MIP1-α/CCL-3 (G), or IP-10 (H) in the culture supernatant were evaluated in a multiplex cytokine ELISA as described in Materials and Methods. ELISA data are expressed as means ± SD of values from triplicate experiments that yielded similar results. *, $P < 0.05$; **, $P < 0.005$ compared to WT-infected BMDM.

ine whether live attenuated parasites induced a proinflammatory response in macrophages *in vitro*. We observed that, unlike WT parasite infection, live attenuated parasite infection led to a significant induction of proinflammatory cytokine secretion (TNF-α, IL-12, IFN-γ, and IL-6) from BMDM (Fig. 3A to D) in response to LPS. Importantly, production of the anti-inflammatory cytokine IL-10 in live attenuated parasite-infected BMDM was significantly lower than in WT-infected BMDM and was similar to that in the uninfected control (Fig. 3E). Interestingly, the patterns of proinflammatory cytokine (TNF-α, IFN-γ, and IL-12) (see Fig. S1A to C in the supplemental material) and anti-inflammatory cytokine (IL-10) (see Fig. S1D) production by BMDM infected with add-back parasites were similar to those of BMDM infected with WT parasites in response to LPS or rIFN-γ. Along with the cytokines, chemokines have long been characterized as key elements in mediating protection against *Leishmania* infection (51, 52) and play an important role in amplifying the M1 macrophage response (22). Therefore, we studied the expression of chemokines such as monocyte chemoattractant protein 1 (MCP-1)/CCL-2 (Fig. 3F), macrophage inflammatory protein 1α (MIP-1α)/CCL-3 (Fig. 3G), and IP-10 (Fig. 3H). Comparative chemokine profiles clearly revealed that live attenuated parasite infection induced expression of these chemokines in BMDM compared to WT-infected BMDM (Fig. 3F, G, and H). The results indicated that live attenuated parasites are capable of eliciting strong proinflammatory cytokine and chemokine responses in BMDM compared to WT parasites, suggesting induction of M1 macrophage immunity.

Live attenuated parasite infection induces effector function in BMDM via activation of p38 MAPK. It has been well documented that p38 MAPK signaling is a key regulator of IL-12 and NO production (49, 53). *L. donovani* parasites deactivate the p38 MAPK signaling cascade by inhibiting phosphorylation, thus attenuating macrophage effector function (53). Hence, we explored how live attenuated parasites affect p38 MAPK phosphorylation in BMDM. We found that in live attenuated parasite-infected BMDM, p38 MAPK phosphorylation was higher than that in uninfected or WT-infected BMDM in response to LPS stimulation (Fig. 4A). However, infection with add-back parasites caused a reduced level of p38 MAPK phosphorylation compared to that in live attenuated parasite-infected BMDM. We further analyzed the involvement of p38 MAPK signaling in live attenuated parasite induction of IL-12 and NO production by using a p38 MAPK signaling inhibitor. SB203580 pretreatment of either WT-, live attenuated-, or add-back parasite-infected macrophages significantly abrogated the generation of NO (Fig. 4B) and IL-12 (Fig. 4C) compared to that in untreated BMDM, indicating the involvement of p38 MAPK signaling in the modulation of the proinflammatory response in BMDM by different groups of parasites.

Live attenuated parasite infection does not alter the physiology of macrophage membranes. Cholesterol is one of the major

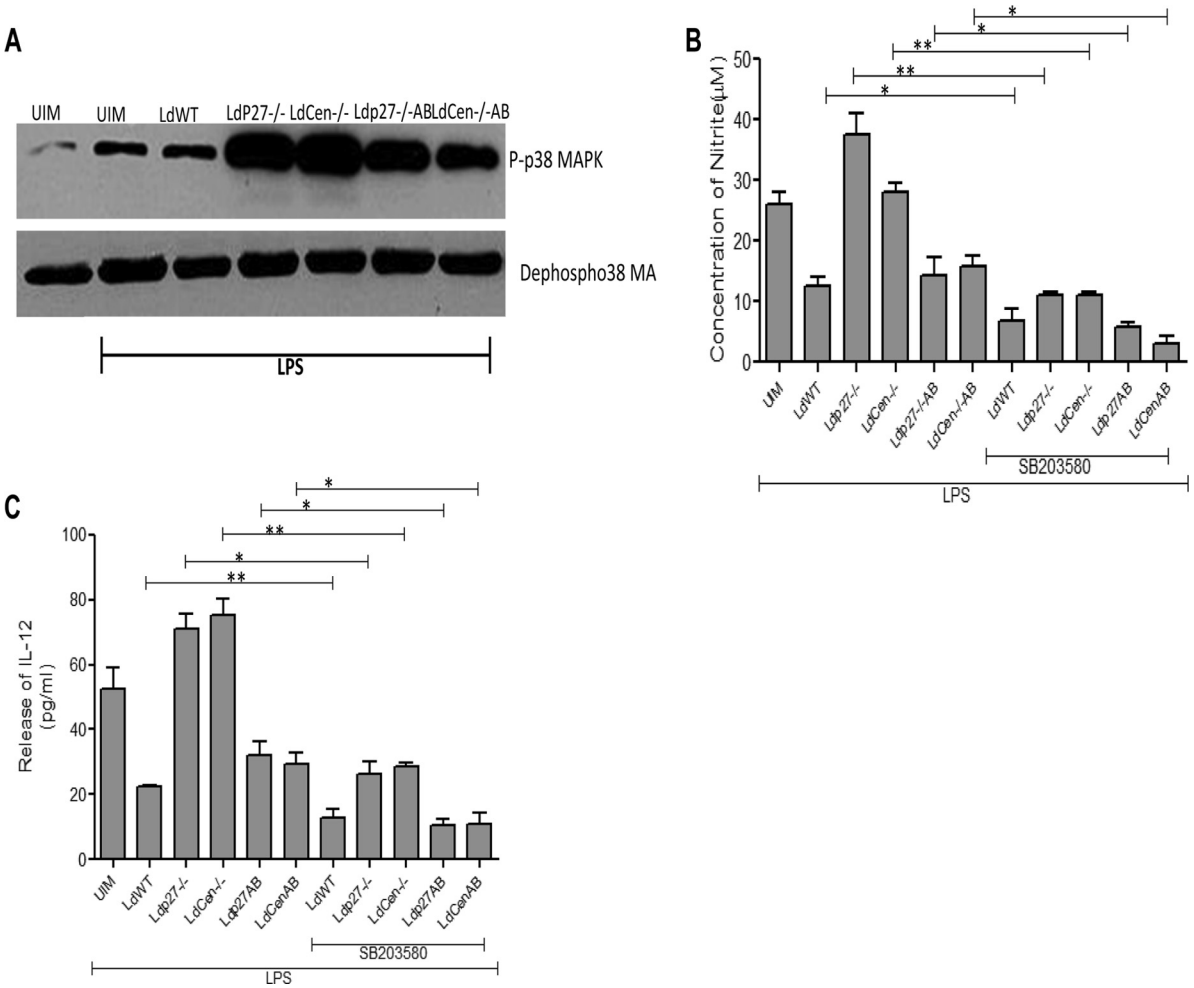

FIG 4 Live attenuated parasite infection induces effector function in BMDM via p38 MAPK activation. (A) BMDM were either left uninfected or infected with various groups of parasites for 2 h. Whole-cell lysates were prepared, subjected to Western blotting, and then assessed for p-p38 MAPK and dephospho-p38 MAPK. The results are representative of 3 independent experiments with similar findings. (B and C) In a separate experiment, BMDM were treated with SB203580 (SB; 10 μg/ml) for 2 h. The cells were then infected with either WT, live attenuated, or add-back parasites and stimulated with LPS for 24 h as described above. Culture supernatants were then collected to analyze NO production (B) and IL-12 production (C). The data represent the means ± standard deviations of three independent experiments. *, $P < 0.05$; **, $P < 0.005$.

components in plasma membranes and regulates membrane fluidity (16). *L. donovani*-mediated depletion of macrophage membrane cholesterol after the parasite establishes itself inside the host cell results in defective antigen presentation, leading to the pathogenesis of VL (54). Hence, we first analyzed whether live attenuated parasite infection affected membrane cholesterol in BMDM. Cells were infected with RFP-labeled WT, *Ldp27*$^{-/-}$-RFP, or *LdCen*$^{-/-}$-mCherry promastigotes for 24 h, and the change in cholesterol content was subsequently examined by measuring fluorescence intensity from the cholesterol-labeling probe filipin using confocal microscopy (Fig. 5A). Confocal microscopic analysis showed that uninfected macrophages (UIM) (Fig. 5A, panel a) exhibited bright blue filipin staining. The corresponding six-step intensity profile of the filipin fluorescence from the same images, represented by a 2.5-D graph, also revealed that most of the UIM (Fig. 5A, panel e) were fully loaded with cholesterol, as the fluorescence intensity reached the highest intensity (pink on the intensity scale). However, fluorescent WT-RFP infection (Fig. 5A, panel b, red fluorescent spots) resulted in the removal of membrane cholesterol from BMDM, as indicated by the decrease in filipin fluorescence in the confocal microscopic analysis (Fig. 5A, panel b) and by the filipin intensity in the 2.5-D graph (Fig. 5A, panel f). Interestingly, fluorescent *Ldp27*$^{-/-}$-RFP and *LdCen*$^{-/-}$-mCherry parasite infection (Fig. 5A, panels c and d, red spots) did not quench cholesterol from BMDM, based on confocal microscopic analysis (Fig. 5A, panels c and d). The quantitative comparison of the fluorescence intensities in the 2.5-D graphs from the filipin images revealed that *Ldp27*$^{-/-}$-RFP and *LdCen*$^{-/-}$-mCherry parasite-infected BMDM (Fig. 5A, panels g and h) were fully loaded with cholesterol, as shown by the filipin fluorescence at the highest intensity step (pink on the intensity scale). Additionally, flow cytometry data showed that cholesterol content in BMDM infected with live attenuated parasites (*Ldp27*$^{-/-}$ and *LdCen*$^{-/-}$) was similar to that in uninfected cells, indicating that live attenuated parasites did not deplete cholesterol from BMDM; however, the add-back parasites (*Ldp27*$^{-/-}$AB, *LdCen*$^{-/-}$AB) significantly depleted the cholesterol as represented by the histogram in Fig. 5B and the corresponding quantitative analysis of mean

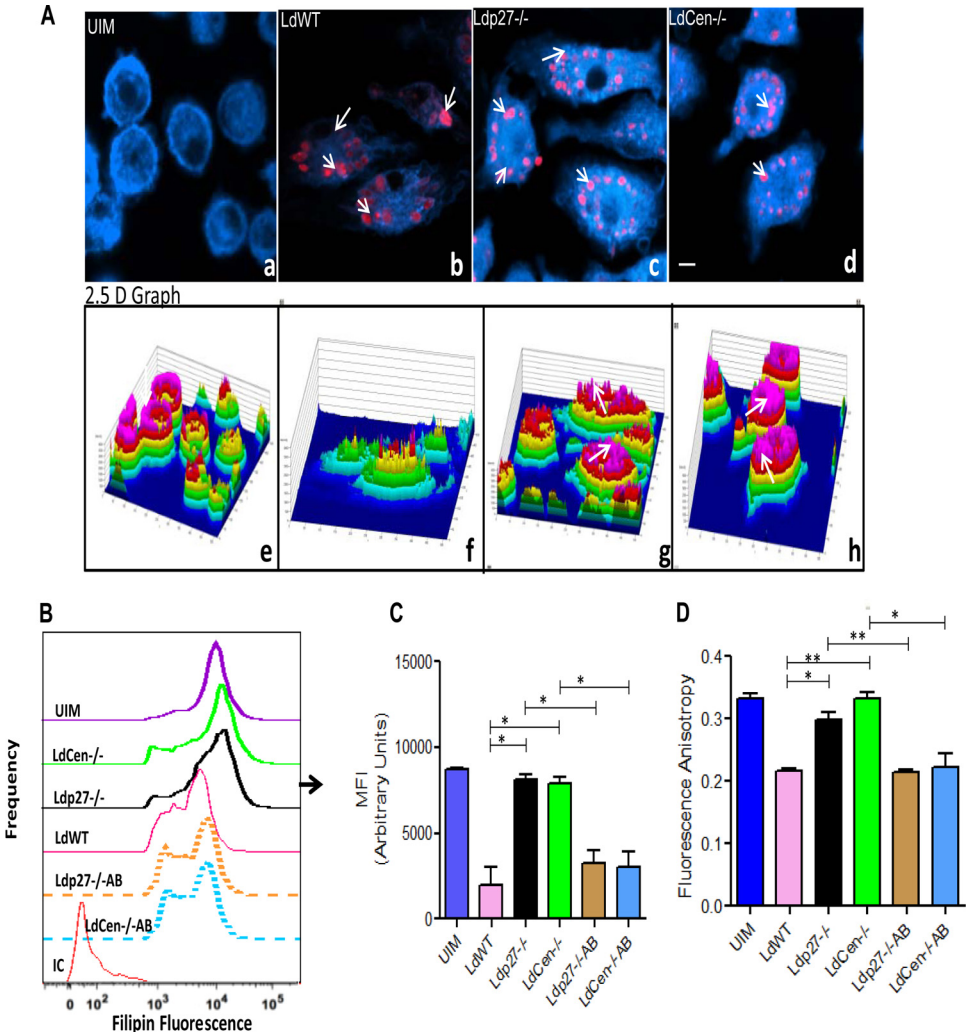

FIG 5 Live attenuated parasite infection does not deplete membrane cholesterol and does not alter membrane fluidity of BMDM. BMDM were either left uninfected or infected with either RFP-tagged WT or RFP-tagged *Ldp27*$^{-/-}$ or mCherry-tagged *LdCen*$^{-/-}$ parasites for 24 h as described in Materials and Methods and then processed for confocal microscopy. (A) Cell preparations were stained with filipin and observed under a confocal laser-scanning microscope. The micrograph is representative of 3 independent experiments in which at least 100 cells per sample were analyzed. Bar, 10 μm. The corresponding filipin fluorescence intensity plots are shown below the respective micrographs, with the fluorescence intensity plotted on the *z* axis (a six-step rainbow look-up table was used to help visualize the range of intensity values within the micrographs). (B and C) In a separate experiment, BMDM were either left uninfected or infected with WT, live attenuated, or add-back parasites for 24 h. Macrophages were then stained with filipin and analyzed by flow cytometry. Control staining with isotype-matched antibodies was negative. Data are from 1 of 3 experiments conducted in the same way with similar results. *, $P < 0.05$; **, $P < 0.005$. (D) BMDM were either left uninfected or infected with various groups of parasites as described above. After 24 h, the membrane fluidity was estimated by calculating the fluorescence anisotropy value. The data represent the mean values ± standard deviations of results from 3 independent experiments that all yielded similar results. *, $P < 0.05$; **, $P < 0.005$.

fluorescence intensity (MFI) for BMDM (Fig. 5C). These results indicated that, unlike BMDM infected with WT parasites, live attenuated parasite-infected BMDM retain the membrane architecture, similar to what is observed in uninfected controls, as no quenching of cholesterol takes place in these cells. Since live attenuated parasites did not quench cholesterol from the infected cell membrane, we analyzed whether live attenuated parasites affected the membrane fluidity of the infected cells by measuring FA using DPH as a probe. FA was significantly diminished 24 h after infection with WT or gene-complemented add-back parasites compared to FA of uninfected macrophages, suggesting enhanced fluidity of the membrane of parasitized BMDM. In contrast, live attenuated parasite-infected BMDM did not alter the FA of the membrane in infected cells, suggesting no change in membrane fluidity (Fig. 5D). Taken together, these data suggest that the live attenuated parasite infection did not affect normal membrane architecture in BMDM, as was observed with WT or add-back parasite infections of such macrophages.

Live attenuated parasite infection enhances antigen presentation in BMDM and induces *in vitro* T cell proliferation. Since we did not observe any change in membrane architecture, i.e., membrane fluidity, in BMDM, we analyzed the antigen-presenting function of the BMDM upon infection with live attenuated parasites. We first analyzed the expression of costimulatory molecules after infection with WT or live attenuated parasites. There was no difference in the expression (MFI) of MHC-II, CD40,

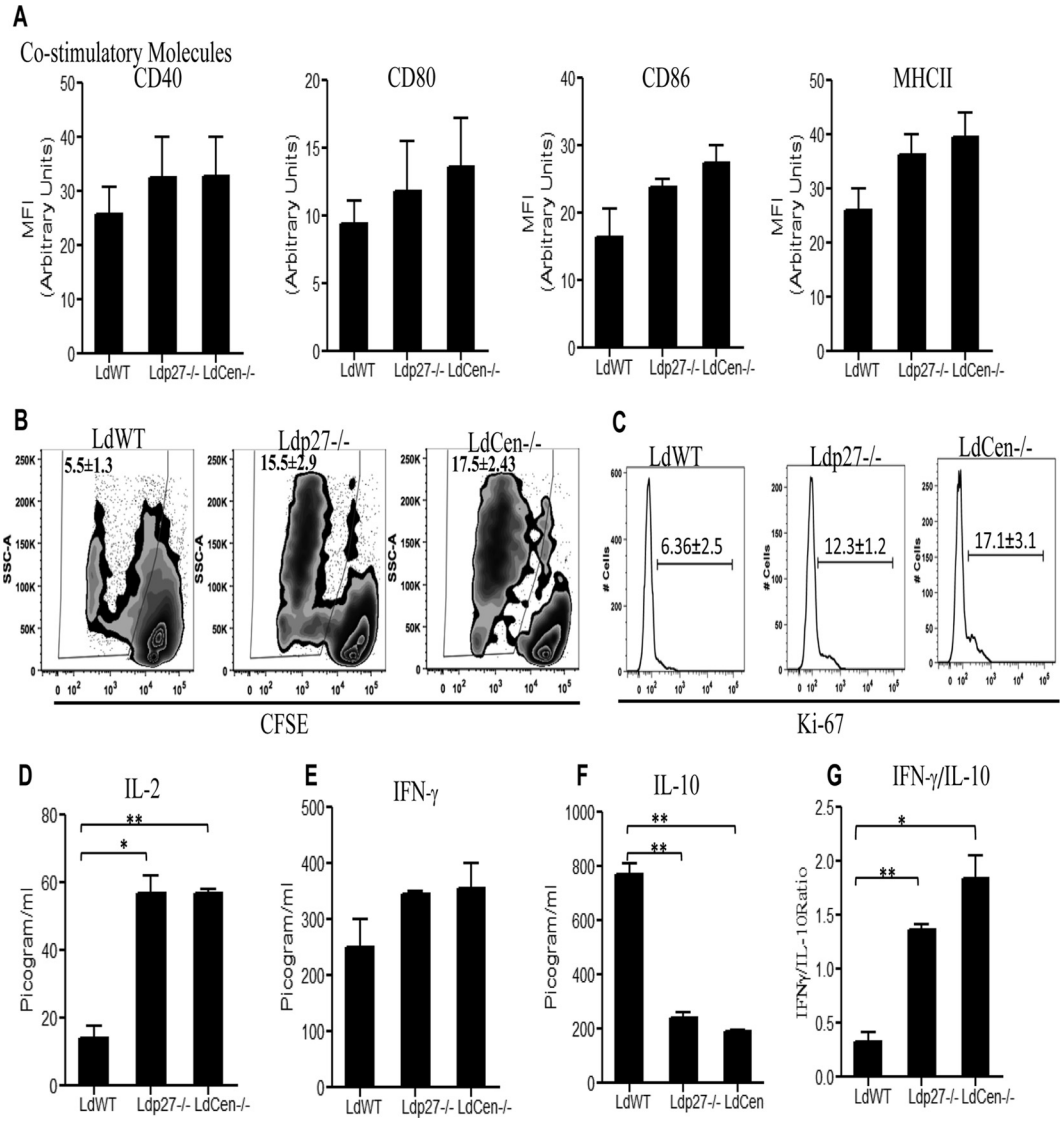

FIG 6 Costimulatory molecule expression and T cell proliferation upon coculture of parasite-infected BMDM with OVA-specific transgenic T cells. (A) BMDM were infected with various groups of parasites as described in Materials and Methods for 24 h. The expression of MHC-II, CD40, CD80, and CD86 on BMDM was studied, and MFI were calculated based on flow cytometry results. (B) BMDM were pulsed with OVA peptide and infected with WT or live attenuated parasites for 24 h and then cocultured with purified CFSE-labeled $CD4^+$ T cells from DO11.10 transgenic mice. CFSE dilution was measured in $CD4^+$-gated T cells pulsed with different leishmanial lines. The experiment was independently repeated three times. (C) In a separate experiment, cell supernatants were collected from BMDM-$CD4^+$ T cell coculture sets and stained with anti-Ki67 –PE and anti-CD4–FITC. T cell proliferation was estimated by flow cytometry by gating on $Ki67^+$ $CD4^+$ cells. Representative histograms shown here are from experiments repeated independently for three times. (D to F) Culture supernatants were collected after 5 days of coculture, and cytokines IL-2 (D), IFN-γ (E), and IL-10 (F) were measured using ELISA kits as per the manufacturer's instructions. (G) The IFN-γ/IL-10 ratio was determined. The data represent the mean values ± standard deviations of results from 3 independent experiments. *, $P < 0.05$; **, $P < 0.005$ compared to WT-infected BMDM.

CD80, or CD86 molecules between BMDM infected with WT or live attenuated parasites (Fig. 6A). Next, we investigated the antigen presentation capability of live attenuated parasite-infected BMDM by evaluating their ability to present live attenuated parasite antigens to CFSE-labeled naive $CD4^+$T cells. BMDM infected with WT or live attenuated parasites were pulsed with OVA peptide ($OVA_{323–339}$) and then cocultured with OVA-specific (DO11.10) CFSE-labeled $CD4^+$ cells. $CD4^+$ T cell proliferation was evaluated after 5 days by flow cytometry. Live attenuated parasite infection of BMDM induced proliferation of T cells, based on the significantly higher percentage of proliferating $CD4^+$ T cells compared to those cocultured with WT-infected BMDM (Fig. 6B). We also independently confirmed that live attenuated parasite infection induced $CD4^+$ T cell proliferation, based on the expression of Ki67, a cellular marker for proliferation which is expressed exclusively in proliferating cells (Fig. 6C). Based on the expression of Ki67, both *Ldp27*$^{-/-}$ and *LdCen*$^{-/-}$ parasites induced more $CD4^+$ T cell proliferation than WT parasites (Fig. 6C). Cytokine production resulting from a $CD4^+$ T cell response was measured in culture supernatants after 7 days of coculture. Live attenuated parasite-infected BMDM-T cell cocultures showed a significant increase in IL-2 production (Fig. 6D) and

higher levels of IFN-γ (Fig. 6E) than those with WT infection. On the other hand, live attenuated parasite-infected OVA-pulsed BMDM-T cell cocultures had significantly reduced IL-10 production compared to WT-infected BMDM (Fig. 6F). Overall, the IFN-γ/IL-10 ratio was significantly higher in live attenuated parasite-infected, OVA-pulsed BMDM-T cell cocultures than in those with WT infection (Fig. 6G). Thus, these results suggest that live attenuated parasite-infected BMDM are capable of inducing the proliferation of Th1 type $CD4^+$ T cells *in vitro*, and the findings are consistent with an enhanced adaptive immune response to live attenuated parasites in various animal models as has been demonstrated elsewhere (40–43).

Live attenuated parasite infection in mice induces classical activation (M1 phenotype) of parasitized macrophages isolated from spleens. Since highly phagocytic splenic macrophages play a pivotal role in regulating the killing of intracellular *L. donovani* (55), we next assessed the ability of live attenuated parasites to modulate the macrophage response in spleens in an *in vivo* mouse model. We infected mice via the tail vein with WT-RFP, *LdP27*$^{-/-}$-RFP, or *LdCen*$^{-/-}$- mCherry parasites. After 7 days of infection, sorting of UIM from the spleens from the different groups of mice was done by gating live single cells for lineage$^-$ (T cell, B cell, NK cell) RFP^- $Cd11b^+$ MHC-II^+ $Cd11c^-$ $Ly6G^-$, whereas parasitized macrophages (IM) were sorted by gating live single cells for lineage$^-$ (T cell, B cell, NK cell) RFP^+ $Cd11b^+$ MHC-II^+ $Cd11c^-$ $Ly6G^-$ (Fig. 7A). Consistent with our *in vitro* infection data, live attenuated parasite-infected mice had significantly lower splenic parasite burdens than WT-infected mice (Fig. 7B).

To further characterize the polarization of parasitized splenic macrophages toward either the classical (M1) phenotype or alternative (M2) phenotype, we assessed the expression levels of well-studied (56) M1 and M2 markers in the infected macrophage populations and compared them with those in WT-parasitized macrophages. RT-PCR analysis showed that 4 major M1 markers, iNOS2 (Fig. 7C, panel a), IL-1β (Fig. 7C, panel b), TNF-α (Fig. 7C, panel c), and IL-12 (Fig. 7C, panel d), were significantly elevated in parasitized splenic macrophages isolated from live attenuated parasite-infected mice compared to WT-infected mice. In contrast, 4 major M2 markers, Arg-1(Fig. 7C, panel e), MRC-1(Fig. 7C, panel f), YM1 (Fig. 7C, panel g), and IL-10 (Fig. 7C, panel h), were significantly reduced in parasitized macrophages isolated from live attenuated parasite-infected mice compared to WT-infected mice. Interestingly, UIM from live attenuated parasite-infected mice showed slightly higher levels, not statistically significant, of IL-1β (Fig. 7C, panel b) and IL-12 (Fig. 7C, panel d), along with downregulation of the M2 macrophage-specific Arg-1(Fig. 7C, panel e), MRC-1 (Fig. 7C, panel f), YM1(Fig. 7C, panel g), and IL-10 (Fig. 7C, panel h) genes compared to uninfected macrophages from WT-infected mice. Therefore, it seems that the infection with live attenuated parasites generates a bystander effect. Thus, from the *in vivo* gene expression profile, it is also evident that live attenuated parasite infection promotes a state of classical activation in splenic macrophages.

BMDM from live attenuated parasite-infected mice are more efficient antigen-presenting cells (APC) than those from WT-infected mice. IL-12 is a critical cytokine that skews the development of naive $CD4^+$ T cells into Th1 cells (4). To determine if the higher IL-12 production of live attenuated parasite-infected macrophages affects their ability to activate naive T cells, we isolated BMDM from WT-infected or live attenuated parasite-infected mice 7 days postinfection. We pulsed these BMDM with OVA peptide ($Ova_{323–339}$) followed by coculture with OVA-specific $CD4^+$ T cells for 5 days to analyze OVA-specific proliferation of T cells. Interestingly, and consistent with our *in vitro* study results, the percentage of proliferating $CD4^+$ T cells after 5 days was comparatively higher upon coculture with OVA-pulsed BMDM from live attenuated parasite-infected mice versus WT-infected mice, as illustrated in Fig. 8A by the offset histogram depicting the individual percentage of proliferating $CD4^+$ T cells from the different groups. Cytokine production resulting from such a $CD4^+$ T cell response was measured in culture supernatants after 5 days of coculture. The results showed that BMDM from live attenuated parasite-infected mice stimulated $CD4^+$ T cells to produce significantly higher levels of IL-2 and IFN-γ than those from WT-infected controls (Fig. 8B). In contrast, BMDM from live attenuated parasite-infected mice, upon coculture with T cells, had significantly lower IL-10 production than those from WT-infected mice (Fig. 8B). Overall, $CD4^+$ T cells cocultured with BMDM from live attenuated parasite-infected mice displayed significantly higher IFN-γ/IL-10 ratios than $CD4^+$ T cells cocultured with BMDM from WT-infected mice (Fig. 8C), thereby indicating a Th1 response predominance that could account for further protective immunity.

DISCUSSION

Impairment in both the proinflammatory cytokine response and the generation of free radicals during VL helps the *L. donovani* to establish itself within the hostile environment of macrophages (57). Although dendritic cells are involved in the initial priming of the antileishmanial immune response and may sustain short-term survival of *Leishmania* parasites, macrophages are the major site for *Leishmania* parasite replication (58). Recent evidence suggests that the ability of macrophages to process and present *Leishmania* antigens is necessary for their efficient interaction with effector T cells and subsequent activation of the adaptive immune response (58). Furthermore, recent studies indicated that macrophage-directed adaptive immunity is often a combination of M1/Th1 and M2/Th2 responses (56, 59, 60). M1 phenotype macrophages preferentially express iNOS and direct T cells to produce Th1-like cytokines. In contrast, M2 macrophages preferentially express arginase and stimulate T cells to produce Th2-like cytokines. Thus, macrophages control immunologic outcomes on their own and subsequently direct the T cell response (27, 31). For example, *Leishmania* infection of macrophages increases their ability to stimulate a parasite-favorable Th2 response instead of a host-protective Th1 response (44). Consequently, the outcome of *Leishmania* infection depends to a large extent on the interplay between the parasites and the macrophages.

Previous studies from our laboratory showed, by using a few genetically modified *L. donovani* parasites (*LdCen*$^{-/-}$ or *Ldp27*$^{-/-}$), induction of a host-protective Th1 adaptive immune response and long-term protection against *L. donovani* infection (40–43). However, whether the immunological basis of protection in terms of the host innate response induced by these live attenuated parasites could account for the protection observed in various animal models (40–43) remains unexplored. Hence, in this report we explored the early immune responses, especially macrophage functions, in determining the extent of the Th1 adaptive immune response.

We found that live attenuated parasites could not persist as

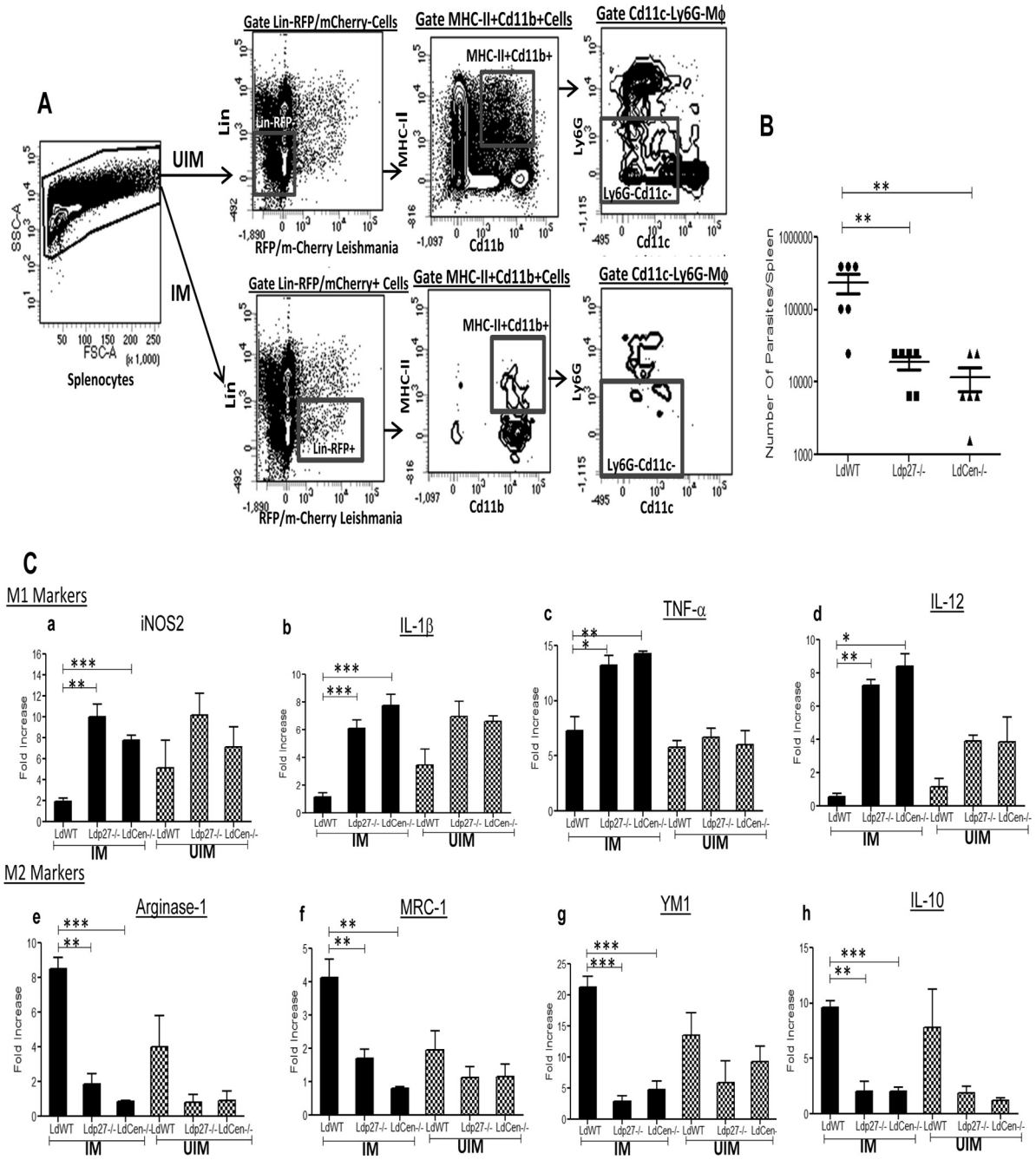

FIG 7 Live attenuated parasite infection in mice induces classical activation (M1 phenotype) of parasitized macrophages isolated from spleens. (A) UIM were sorted from the spleens of different groups of mice ($n = 6$) by gating live single cells for lineage$^-$ (T cell, B cell, NK cell) RFP/mCherry$^-$ Cd11b$^+$ MHCII$^+$ Cd11c$^-$ Ly6G$^-$) markers, whereas parasitized splenic macrophages (IM) were sorted by gating live single cells for lineage$^-$ (T cell, B cell, NK cell) RFP/mCherry$^+$ Cd11b$^+$ MHC-II$^+$ Cd11c$^-$ Ly6G$^-$) markers. The sorting strategy is displayed. The experiment was repeated 3 times with pooled digests from 6 spleens per experiment. (B) Parasite numbers in spleens of different groups of infected mice were measured 7 days postinfection. Means and standard errors of the means for six mice in each group are shown. Data are representative of two independent experiments. **, $P < 0.005$. (C) Sorted parasitized and uninfected macrophages from different groups of mice were subjected to RNA isolation as described in Material and Methods. Isolated total RNA was reverse transcribed and expression levels of different genes were analyzed as described in Material and Methods. Normalized expression levels of M1 markers, such as iNOS2, IL-1β, TNF-α, and IL-12, and M2 markers like Arg-1, MRC-1, YM1, and IL-10 were estimated. The data represent the mean values ± standard deviations of results from 3 independent experiments that all yielded similar results.*, $P < 0.05$; **, $P < 0.005$; ***, $P < 0.0005$ compared to WT-infected BMDM.

long as WT parasites. Interestingly, replication in macrophages was restored to near-wild-type virulence levels in gene-complemented add-back parasites (*Ldp27*$^{-/-}$AB and *LdCen*$^{-/-}$AB), specifically implying that the difference in infectivity is a direct consequence of *Ldp27* or *Centrin1* deficiency in the *Ldp27*$^{-/-}$ and *LdCen*$^{-/-}$ parasites, respectively. These findings are consistent with our earlier studies in human macrophages and in mice (35, 40).

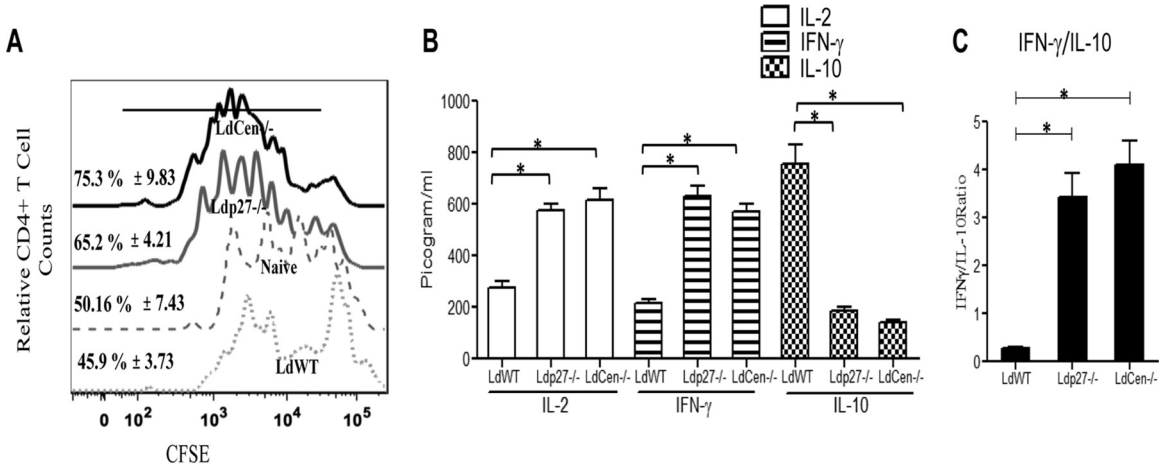

FIG 8 BMDM from live attenuated parasite-infected mice are more efficient antigen-presenting cells than BMDM from WT-infected mice. BMDM isolated from BALB/c mice either uninfected or infected for 7 days with WT or live attenuated parasites were pulsed with OVA peptide and then cocultured with purified CFSE-labeled $CD4^+$ T cells from DO11.10 transgenic mice. T cell proliferation was estimated by flow cytometry by studying CFSE dilution of gated $CD4^+$ cells and is represented by the histogram. The staggered offset histogram overlay (A) displays the $CD4^+$ T cell proliferation pattern as visualized by CFSE dilution after flow cytometry. (A) Cell proliferation was analyzed in triplicate experiments, and histograms representative of mean values were overlaid for the figure. The black bold line on the histogram overlay represents the percentage of proliferating $CD4^+$ T cells. (B) The culture supernatant fluids were collected and assayed for IL-2, IFN-γ, and IL-10 in an ELISA. (C) The IFN-γ/IL-10 ratio was calculated from the data shown in panel B. The data represent the picogram levels of cytokines in culture supernatants and are presented as means ± standard deviations from three independent experiments. *, $P < 0.05$ compared to WT-infected BMDM.

Macrophage activation for enhanced microbial activity is a critical requirement, as it leads to the successful elimination of *Leishmania* parasites. The ability of macrophages to secrete ROS, as well as reactive nitrogen intermediates (RNI), correlates closely with their capacity to kill *Leishmania* parasites (6–8), and these abilities are hallmarks of the classical activation (M1) macrophage phenotype (4, 17). ROS-mediated killing is predominantly an early event, whereas NO-mediated clearance of parasites occurs at a later stage in the infection (48). We found markedly elevated ROS generation in live attenuated parasite-infected BMDM compared to WT-parasitized BMDM. Moreover, we observed enhanced NO generation along with higher iNOS2 expression in live attenuated parasite-infected BMDM in response to either LPS or rIFN-γ stimulation, thereby indicating that live attenuated parasites do not inhibit the microbicidal activity of macrophages and, subsequently, their impaired growth inside BMDM. Recent evidence indicated that iNOS is recruited to the membranes of parasitophorous vacuoles (PV), and several infectious microorganisms, such as *Mycobacteria* spp. and *Salmonella* spp. inhibit iNOS recruitment to PV during macrophage infection, attenuating NO production, which eventually plays a role in the pathogenesis of these bacteria (61, 62). In our study, we found that live attenuated parasite infection induced enhanced iNOS2 in response to LPS in the vicinity of the PV of the BMDM, indicating higher production of NO. Further, Th2 cytokine-induced enhanced host arginase activity during *Leishmania* infection is associated with depletion of L-arginine availability, thereby resulting in reduced levels of NO and enhanced production of polyamines for parasite survival (10, 12, 63). In contrast, another study group has shown that *Leishmania major* encodes arginase, which itself enhances disease pathogenesis by augmenting host cellular arginase activities in a parasite number-dependent manner (64). In our study, we found that live attenuated parasites were unable to replicate and suppressed anti-inflammatory or Th2 cytokine production in BMDM, thereby downregulating the arginase-1 activity compared to results after WT infection in response to either LPS or rIFN-γ stimulation. Taken together, upregulated expression of iNOS2, a hallmark of classical activation, and downregulated expression/activity of arginase-1, the hallmark of alternative activation, by live attenuated parasite-infected macrophages upon LPS or rIFN-γ stimulation suggest that, unlike WT parasites, live attenuated parasites induce the classical (M1) macrophage phenotype and enhance microbicidal activity.

Disruption of macrophage activation during *L. donovani* infection involves parasite-mediated skewing of proinflammatory cytokine synthesis toward anti-inflammatory cytokines that suppress the killing capacities of macrophages (65). In this context, the most important mechanism analyzed to date appears to be the inhibition of IL-12 synthesis in parasitized cells, which subsequently delays or prevents the secretion of another important proinflammatory cytokine, IFN-γ, from $CD4^+$ Th1 cells; IFN-γ is a major inducer of classical activation of macrophages (4). Moreover, it has been shown that IL-10, an anti-inflammatory cytokine, perturbs classical macrophage activation by attenuating the respiratory burst and inflammatory cytokine production, particularly of IL-12 and TNF-α by macrophages, hence promoting parasite survival (4). Since IL-12 is a critical proinflammatory cytokine required for $CD4^+$ Th1 development and production of IFN-γ (4, 23), it is evident that live attenuated parasite infection-induced IL-12 in macrophages subsequently helps in the generation of a protective Th1 response, as observed in our previous *in vivo* studies (40–43). In addition, live attenuated parasite infection was able to downregulate the anti-inflammatory cytokine IL-10 production in BMDM. Thus, this efficient regulation of pro- and anti-inflammatory cytokines by live attenuated parasites might regulate the generation of NO in BMDM, which may eventually activate macrophage effector functions (66). Of note, both proinflammatory (TNF-α, IL-12, and IFN-γ) and anti-inflammatory (IL-10) cytokine production approached WT levels in add-back parasite-infected macrophages in response to either

LPS or rIFN-γ. These data indicate that the increased proinflammatory response and attenuated anti-inflammatory response by *Ldp27*$^{-/-}$ or *LdCen*$^{-/-}$ parasite infection is related to a deficiency of the *Ldp27* or *Centrin1* gene, respectively.

Successful immunity to *Leishmania* depends on recruitment of appropriate immune effector cells to the site of infection, and chemokines play a crucial role in this process (52). Specifically, *in vitro* studies with the chemokine CCL2 (MCP-1) demonstrated its ability to synergize with IFN-γ and subsequently induce antileishmanial activity in macrophages, which may potentially kill *Leishmania* and promote healing (52). Additionally, recent evidence also suggests that MCP-1/CCL2 plays a pivotal role in the amplification of the M1-type macrophage response (22). We observed that live attenuated parasite infection significantly induced chemokines, such as MCP-1/CCL-2, MIP-1α/CCL-3, and IP-10, further indicating chemokine-mediated activation of macrophages. Thus, our *in vitro* study clearly indicated that, in contrast to WT infection, live attenuated parasite infection induces classical activation of macrophages, as indicated by inhibition of arginase-1 and IL-10 production and concomitant induction of iNOS2, IL-12, TNF-α, MCP-1/CCL-2, MIP-1α/CCL-3, and IP-10 release, which may subsequently translate into an *in vivo* protective response, as shown in our previous *in vivo* studies (40–43).

The macrophage activation is controlled through signaling via p38 MAPK phosphorylation (53), and *Leishmania* infection inhibits macrophage-mediated IL-12 and NO production by attenuating p38 MAPK phosphorylation (67). We found that live attenuated parasite infection induced p38 MAPK phosphorylation in BMDM, contrary to what is seen with WT infection. Further, inhibition of p38 MAPK resulted in impaired NO and IL-12 production in live attenuated parasite-infected BMDM. Thus, it is apparent that the activation of p38 MAPK signaling at early time points in infection is intricately associated with the production of proinflammatory molecules in live attenuated parasite-infected BMDM.

L. donovani infection results in defective antigen presentation by macrophages to T cells (15), thereby attenuating the generation of an effective cell-mediated immune response. The defective antigen-presenting ability of infected macrophages closely correlates with alterations in the physical properties of macrophage cell membranes and has been proposed as a mechanism employed by the parasite to evade the host immune system (68). Specifically, the role of membrane cholesterol in APC and T cell interactions has been well studied in VL (16). Similar effects were observed with *L. major* infection-mediated depletion of membrane cholesterol, resulting in the disruption of macrophage effector functions; more interestingly, cholesterol loading augments the microbicidal effect in macrophages (69). Recently it was shown that liposomal cholesterol delivery activates the macrophage innate immune arm to facilitate intracellular *L. donovani* killing (48). Further, the cholesterol content of the macrophage membrane regulates membrane fluidity of macrophages, which has a significant bearing on T cell-stimulating ability (16). In our study, unlike infection with WT parasites, live attenuated parasite infection neither depleted cholesterol from macrophage membranes nor changed membrane fluidity, suggesting that live attenuated parasite infection did not alter macrophage membrane architecture. However, similar to WT parasites, add-back parasites quenched the membrane cholesterol and increased the membrane fluidity, thereby reversing the effects of live attenuated parasites on the membrane. Taken together, these results suggest that live attenuated parasite (*Ldp27*$^{-/-}$ or *LdCen*$^{-/-}$) infection might not impede the normal macrophage membrane architecture and hence may not impair antigen presentation. In fact, the lack of an effect on macrophage membrane architecture in turn resulted in an enhanced antigen presentation capability of OVA-pulsed BMDM infected with live attenuated parasites, compared to those infected with WT parasites, as indicated by OVA-specific proliferation of T cells. Further, such an interaction between BMDM and T cells *in vitro* also resulted in enhanced T cell effector function, as evident from higher IL-2 and IFN-γ and reduced IL-10 release compared to that in WT-infected BMDM. These studies suggest that infection of macrophages *in vitro* with live attenuated parasites leads to classical activation (M1 macrophage phenotype), which then allows efficient antigen presentation that leads to the Th1 type of adaptive response.

The above-mentioned *in vitro* observations with regard to classical activation of macrophages by live attenuated parasites were further confirmed by our *in vivo* experiments. For example, the parasitized splenic macrophages from live attenuated parasite-infected mice at 7 days postinfection exhibited upregulation of genes encoding classical macrophage activation (M1 phenotype), such as genes for iNOS2, IL-1β, TNF-α, and IL-12, and downregulation of genes implicated in alternative macrophage activation (M2 phenotype), such as genes for Arg-1, MRC-1, IL-10, and YM1, compared to those from WT-infected mice, suggesting that live attenuated parasite infection induced an M1 macrophage response *in vivo*. In addition, in our *ex vivo* study we observed that BMDM isolated from live attenuated parasitized mice 7 day postinfection were better activators of test antigen (OVA)-specific CD4$^+$ T cells than those from WT-infected mice, as manifested by increased proliferation of OVA-specific CD4$^+$ T cells. Of interest, the macrophages from live attenuated parasite-infected mice present antigen to naive T cells and help in generation of Th1 cells, as indicated by the high level production of IL-2 and IFN-γ and the significantly smaller amount of IL-10. These studies corroborated our previous findings of Th1-predominant protective immunity in live attenuated parasite-immunized and WT-challenged mice and dogs (40–43). It is worth mentioning here that the macrophage-mediated immune response plays a key role in vaccine protection, as recently observed by various groups working with vaccine candidates, such as recombinant BCG, live attenuated West Nile virus, and live attenuated measles virus, against tuberculosis, WNV infection, and measles, respectively; the response manipulates the macrophage population and provides improved protection by enhancing the macrophage effector response (32–34). Therefore, it is likely that the abundance of classically activated macrophages (M1) in live attenuated parasite-infected mice could serve as a biomarker for effective *Leishmania* vaccines (40–43).

In conclusion, in the present study we have demonstrated the mechanism of induction of an innate response to live attenuated parasites in macrophages both *in vitro* and *in vivo*. The outcome of live attenuated parasite interactions with macrophages is qualitatively and quantitatively different from that with WT parasites. Unlike WT *L. donovani* parasites, live attenuated parasites do not perturb the innate effector function and promote a state of classical activation of macrophages (M1 phenotype). Specifically, we showed that live attenuated parasites promote the interaction of these M1 phenotype macrophages with T cells, altering the early immune response such that the IFN-γ/IL-10 ratio produced by the responding T cells is altered toward a protective immune re-

sponse, further substantiating our previous observations on protective adaptive immune responses (40–43). Thus, in response to infection by live attenuated parasites, the antigen-presenting abilities of macrophages are skewed toward a more effective Th1 predominance that could be accountable for protective adaptive immunity in vaccinated mice. Finally, these studies further affirm that genetically modified live attenuated *L. donovani* parasites should be explored as vaccine candidates against VL.

ACKNOWLEDGMENTS

Funding for these studies was provided by intramural funds and the Critical Path Initiative of the Center for Biologics Evaluation and Research, U.S. Food and Drug Administration.

The findings of this study are an informal communication and represent the authors' own best judgments. These comments do not bind or obligate the FDA.

We thank Sreenivas Gannavaram and Sanjai Kumar for critical review of the manuscript.

REFERENCES

1. **Das A, Ali N.** 2012. Vaccine development against Leishmania donovani. Front Immunol **3:**99. http://dx.doi.org/10.3389/fimmu.2012.00099.
2. **Handman E, Bullen DV.** 2002. Interaction of Leishmania with the host macrophage. Trends Parasitol **18:**332–334. http://dx.doi.org/10.1016/S1471-4922(02)02352-8.
3. **Russell DG, Xu S, Chakraborty P.** 1992. Intracellular trafficking and the parasitophorous vacuole of Leishmania mexicana-infected macrophages. J Cell Sci **103:**1193–1210.
4. **Liu D, Uzonna JE.** 2012. The early interaction of Leishmania with macrophages and dendritic cells and its influence on the host immune response. Front Cell Infect Microbiol **2:**83. http://dx.doi.org/10.3389/fcimb.2012.00083.
5. **Muraille E, Leo O, Moser M.** 2014. TH1/TH2 paradigm extended: macrophage polarization as an unappreciated pathogen-driven escape mechanism? Front Immunol **5:**603. http://dx.doi.org/10.3399/fimmu.2014.00603.
6. **Olivier M, Gregory DJ, Forget G.** 2005. Subversion mechanisms by which Leishmania parasites can escape the host immune response: a signaling point of view. Clin Microbiol Rev **18:**293–305. http://dx.doi.org/10.1128/CMR.18.2.293-305.2005.
7. **Liew FY, Millott S, Parkinson C, Palmer RM, Moncada S.** 1990. Macrophage killing of Leishmania parasite in vivo is mediated by nitric oxide from L-arginine. J Immunol **144:**4794–4797.
8. **Murray HW.** 1982. Cell-mediated immune response in experimental visceral leishmaniasis. II. Oxygen-dependent killing of intracellular Leishmania donovani amastigotes. J Immunol **129:**351–357.
9. **Reiner SL, Locksley RM.** 1995. The regulation of immunity to Leishmania major. Annu Rev Immunol **13:**151–177. http://dx.doi.org/10.1146/annurev.iy.13.040195.001055.
10. **Iniesta V, Gomez-Nieto LC, Corraliza I.** 2001. The inhibition of arginase by N^{ω}-hydroxy-L-arginine controls the growth of Leishmania inside macrophages. J Exp Med **193:**777–784. http://dx.doi.org/10.1084/jem.193.6.777.
11. **Kropf P, Fuentes JM, Fahnrich E, Arpa L, Herath S, Weber V, Soler G, Celada A, Modolell M, Muller I.** 2005. Arginase and polyamine synthesis are key factors in the regulation of experimental leishmaniasis in vivo. FASEB J **19:**1000–1002. http://dx.doi.org/10.1096/fj.04-3416fje.
12. **Iniesta V, Gomez-Nieto LC, Molano I, Mohedano A, Carcelen J, Miron C, Alonso C, Corraliza I.** 2002. Arginase I induction in macrophages, triggered by Th2-type cytokines, supports the growth of intracellular Leishmania parasites. Parasite Immunol **24:**113–118. http://dx.doi.org/10.1046/j.1365-3024.2002.00444.x.
13. **Roberts SC, Tancer MJ, Polinsky MR, Gibson KM, Heby O, Ullman B.** 2004. Arginase plays a pivotal role in polyamine precursor metabolism in Leishmania. Characterization of gene deletion mutants. J Biol Chem **279:**23668–23678. http://dx.doi.org/10.1074/jbc.M402042200.
14. **Noel W, Raes G, Hassanzadeh Ghassabeh G, De Baetselier P, Beschin A.** 2004. Alternatively activated macrophages during parasite infections. Trends Parasitol **20:**126–133. http://dx.doi.org/10.1016/j.pt.2004.01.004.
15. **Chakraborty D, Banerjee S, Sen A, Banerjee KK, Das P, Roy S.** 2005. Leishmania donovani affects antigen presentation of macrophage by disrupting lipid rafts. J Immunol **175:**3214–3224. http://dx.doi.org/10.4049/jimmunol.175.5.3214.
16. **Banerjee S, Ghosh J, Sen S, Guha R, Dhar R, Ghosh M, Datta S, Raychaudhury B, Naskar K, Haldar AK, Lal CS, Pandey K, Das VN, Das P, Roy S.** 2009. Designing therapies against experimental visceral leishmaniasis by modulating the membrane fluidity of antigen-presenting cells. Infect Immun **77:**2330–2342. http://dx.doi.org/10.1128/IAI.00057-09.
17. **Osorio EY, Zhao W, Espitia C, Saldarriaga O, Hawel L, Byus CV, Travi BL, Melby PC.** 2012. Progressive visceral leishmaniasis is driven by dominant parasite-induced STAT6 activation and STAT6-dependent host arginase 1 expression. PLoS Pathog **8:**e1002417. http://dx.doi.org/10.1371/journal.ppat.1002417.
18. **Gordon S.** 2003. Alternative activation of macrophages. Nat Rev Immunol **3:**23–35. http://dx.doi.org/10.1038/nri978.
19. **Rodriguez NE, Chang HK, Wilson ME.** 2004. Novel program of macrophage gene expression induced by phagocytosis of Leishmania chagasi. Infect Immun **72:**2111–2122. http://dx.doi.org/10.1128/IAI.72.4.2111-2122.2004.
20. **Lopes MF, Costa-da-Silva AC, DosReis GA.** 2014. Innate immunity to Leishmania infection: within phagocytes. Mediators Inflamm **2014:**754965. http://dx.doi.org/10.1155/2014/754965.
21. **Edwards JP, Zhang X, Frauwirth KA, Mosser DM.** 2006. Biochemical and functional characterization of three activated macrophage populations. J Leukoc Biol **80:**1298–1307. http://dx.doi.org/10.1189/jlb.0406249.
22. **Mills CD, Ley K.** 2014. M1 and M2 macrophages: the chicken and the egg of immunity. J Innate Immun **6:**716–726. http://dx.doi.org/10.1159/000364945.
23. **Chehimi J, Trinchieri G.** 1994. Interleukin-12: a bridge between innate resistance and adaptive immunity with a role in infection and acquired immunodeficiency. J Clin Immunol **14:**149–161. http://dx.doi.org/10.1007/BF01533364.
24. **Bacellar O, D'Oliveira A, Jr, Jeronimo S, Carvalho EM.** 2000. IL-10 and IL-12 are the main regulatory cytokines in visceral leishmaniasis. Cytokine **12:**1228–1231. http://dx.doi.org/10.1006/cyto.2000.0694.
25. **Gorak PM, Engwerda CR, Kaye PM.** 1998. Dendritic cells, but not macrophages, produce IL-12 immediately following Leishmania donovani infection. Eur J Immunol **28:**687–695. http://dx.doi.org/10.1002/(SICI)1521-4141(199802)28:02<687::AID-IMMU687>3.0.CO;2-N.
26. **Leon B, Lopez-Bravo M, Ardavin C.** 2007. Monocyte-derived dendritic cells formed at the infection site control the induction of protective T helper 1 responses against Leishmania. Immunity **26:**519–531. http://dx.doi.org/10.1016/j.immuni.2007.01.017.
27. **Mills CD, Kincaid K, Alt JM, Heilman MJ, Hill AM.** 2000. M-1/M-2 macrophages and the Th1/Th2 paradigm. J Immunol **164:**6166–6173. http://dx.doi.org/10.4049/jimmunol.164.12.6166.
28. **Cassol E, Cassetta L, Alfano M, Poli G.** 2010. Macrophage polarization and HIV-1 infection. J Leukoc Biol **87:**599–608. http://dx.doi.org/10.1189/jlb.1009673.
29. **Goerdt S, Politz O, Schledzewski K, Birk R, Gratchev A, Guillot P, Hakiy N, Klemke CD, Dippel E, Kodelja V, Orfanos CE.** 1999. Alternative versus classical activation of macrophages. Pathobiology **67:**222–226. http://dx.doi.org/10.1159/000028096.
30. **Mantovani A, Sica A, Sozzani S, Allavena P, Vecchi A, Locati M.** 2004. The chemokine system in diverse forms of macrophage activation and polarization. Trends Immunol **25:**677–686. http://dx.doi.org/10.1016/j.it.2004.09.015.
31. **Rath M, Muller I, Kropf P, Closs EI, Munder M.** 2014. Metabolism via arginase or nitric oxide synthase: two competing arginine pathways in macrophages. Front Immunol **5:**532. http://dx.doi.org/10.3389/fimmu.2014.00532.
32. **Saiga H, Nieuwenhuizen N, Gengenbacher M, Koehler A, Schuerer S, Moura-Alves P, Wagner I, Mollenkopf H, Dorhoi A, Kaufmann SH.** 2014. The recombinant BCG ΔureC::hly vaccine targets the AIM2 inflammasome to induce autophagy and inflammation. J Infect Dis **211:**1831–1841. http://dx.doi.org/10.1093/infdis/jiu675.
33. **Xie G, Luo H, Tian B, Mann B, Bao X, McBride J, Tesh R, Barrett AD, Wang T.** 2015. A West Nile virus NS4B-P38G mutant strain induces cell intrinsic innate cytokine responses in human monocytic and macrophage cells. Vaccine **33:**869–878. http://dx.doi.org/10.1016/j.vaccine.2014.12.056.
34. **Rennick LJ, de Vries RD, Carsillo TJ, Lemon K, van Amerongen G, Ludlow M, Nguyen DT, Yuksel S, Verburgh RJ, Haddock P, McQuaid S, Duprex WP, de Swart RL.** 2015. Live-attenuated measles virus vaccine

targets dendritic cells and macrophages in muscle of nonhuman primates. J Virol **89:**2192–2200. http://dx.doi.org/10.1128/JVI.02924-14.
35. **Dey R, Meneses C, Salotra P, Kamhawi S, Nakhasi HL, Duncan R.** 2010. Characterization of a Leishmania stage-specific mitochondrial membrane protein that enhances the activity of cytochrome c oxidase and its role in virulence. Mol Microbiol **77:**399–414. http://dx.doi.org/10.1111/j.1365-2958.2010.07214.x.
36. **Selvapandiyan A, Debrabant A, Duncan R, Muller J, Salotra P, Sreenivas G, Salisbury JL, Nakhasi HL.** 2004. Centrin gene disruption impairs stage-specific basal body duplication and cell cycle progression in Leishmania. J Biol Chem **279:**25703–25710. http://dx.doi.org/10.1074/jbc.M402794200.
37. **Silvestre R, Cordeiro-da-Silva A, Ouaissi A.** 2008. Live attenuated Leishmania vaccines: a potential strategic alternative. Arch Immunol Ther Exp (Warsz) **56:**123–126. http://dx.doi.org/10.1007/s00005-008-0010-9.
38. **Ravindran R, Ali N.** 2004. Progress in vaccine research and possible effector mechanisms in visceral leishmaniasis. Curr Mol Med **4:**697–709. http://dx.doi.org/10.2174/1566524043360212.
39. **Gannavaram S, Dey R, Avishek K, Selvapandiyan A, Salotra P, Nakhasi HL.** 2014. Biomarkers of safety and immune protection for genetically modified live attenuated leishmania vaccines against visceral leishmaniasis: discovery and implications. Front Immunol **5:**241. http://dx.doi.org/10.3389/fimmu.2014.00241.
40. **Selvapandiyan A, Dey R, Nylen S, Duncan R, Sacks D, Nakhasi HL.** 2009. Intracellular replication-deficient Leishmania donovani induces long-lasting protective immunity against visceral leishmaniasis. J Immunol **183:**1813–1820. http://dx.doi.org/10.4049/jimmunol.0900276.
41. **Dey R, Dagur PK, Selvapandiyan A, McCoy JP, Salotra P, Duncan R, Nakhasi HL.** 2013. Live attenuated Leishmania donovani p27 gene knockout parasites are nonpathogenic and elicit long-term protective immunity in BALB/c mice. J Immunol **190:**2138–2149. http://dx.doi.org/10.4049/jimmunol.1202801.
42. **Fiuza JA, Santiago Hda C, Selvapandiyan A, Gannavaram S, Ricci ND, Bueno LL, Bartholomeu DC, Correa-Oliveira R, Nakhasi HL, Fujiwara RT.** 2013. Induction of immunogenicity by live attenuated Leishmania donovani centrin deleted parasites in dogs. Vaccine **31:**1785–1792. http://dx.doi.org/10.1016/j.vaccine.2013.01.048.
43. **Fiuza JA, Gannavaram S, da Costa Santiago H, Selvapandiyan A, Souza DM, Araújo Passos LS, de Mendonca LZ, Lemos-Giunchetti DDS, Ricci ND, Bartholomeu DC, Giunchetti RC, Bueno LL, Correa-Oliveira R, Nakhasi HL, Fujiwara RT.** 2015. Vaccination using live attenuated Leishmania donovani centrin deleted parasites induces protection in dogs against Leishmania infantum. Vaccine **33:**280–288. http://dx.doi.org/10.1016/j.vaccine.2014.11.039.
44. **Chakkalath HR, Titus RG.** 1994. Leishmania major-parasitized macrophages augment Th2-type T cell activation. J Immunol **153:**4378–4387.
45. **Chagas AC, Oliveira F, Debrabant A, Valenzuela JG, Ribeiro JM, Calvo E.** 2014. Lundep, a sand fly salivary endonuclease increases Leishmania parasite survival in neutrophils and inhibits XIIa contact activation in human plasma. PLoS Pathog **10:**e1003923. http://dx.doi.org/10.1371/journal.ppat.1003923.
46. **Selvapandiyan A, Duncan R, Debrabant A, Bertholet S, Sreenivas G, Negi NS, Salotra P, Nakhasi HL.** 2001. Expression of a mutant form of Leishmania donovani centrin reduces the growth of the parasite. J Biol Chem **276:**43253–43261. http://dx.doi.org/10.1074/jbc.M106806200.
47. **Weischenfeldt J, Porse B.** 2008. Bone marrow-derived macrophages (BMM): isolation and applications. CSH Protoc **2008:**pdb.prot5080. http://dx.doi.org/10.1101/pdb.prot5080.
48. **Ghosh J, Guha R, Das S, Roy S.** 2014. Liposomal cholesterol delivery activates the macrophage innate immune arm to facilitate intracellular Leishmania donovani killing. Infect Immun **82:**607–617. http://dx.doi.org/10.1128/IAI.00583-13.
49. **Bhattacharya P, Gupta G, Majumder S, Adhikari A, Banerjee S, Halder K, Majumdar SB, Ghosh M, Chaudhuri S, Roy S, Majumdar S.** 2011. Arabinosylated lipoarabinomannan skews Th2 phenotype towards Th1 during Leishmania infection by chromatin modification: involvement of MAPK signaling. PLoS One **6:**e24141. http://dx.doi.org/10.1371/journal.pone.0024141.
50. **Rose S, Misharin A, Perlman H.** 2012. A novel Ly6C/Ly6G-based strategy to analyze the mouse splenic myeloid compartment. Cytometry A **81:**343–350. http://dx.doi.org/10.1002/cyto.a.22012.
51. **Teixeira MJ, Teixeira CR, Andrade BB, Barral-Netto M, Barral A.** 2006. Chemokines in host-parasite interactions in leishmaniasis. Trends Parasitol **22:**32–40. http://dx.doi.org/10.1016/j.pt.2005.11.010.
52. **Oghumu S, Lezama-Davila CM, Isaac-Marquez AP, Satoskar AR.** 2010. Role of chemokines in regulation of immunity against leishmaniasis. Exp Parasitol **126:**389–396. http://dx.doi.org/10.1016/j.exppara.2010.02.010.
53. **Junghae M, Raynes JG.** 2002. Activation of p38 mitogen-activated protein kinase attenuates Leishmania donovani infection in macrophages. Infect Immun **70:**5026–5035. http://dx.doi.org/10.1128/IAI.70.9.5026-5035.2002.
54. **Sen S, Roy K, Mukherjee S, Mukhopadhyay R, Roy S.** 2011. Restoration of IFN-γR subunit assembly, IFN-γ signaling and parasite clearance in Leishmania donovani-infected macrophages: role of membrane cholesterol. PLoS Pathog **7:**e1002229. http://dx.doi.org/10.1371/journal.ppat.1002229.
55. **Phillips R, Svensson M, Aziz N, Maroof A, Brown N, Beattie L, Signoret N, Kaye PM.** 2010. Innate killing of Leishmania donovani by macrophages of the splenic marginal zone requires IRF-7. PLoS Pathog **6:**e1000813. http://dx.doi.org/10.1371/journal.ppat.1000813.
56. **Murray PJ, Wynn TA.** 2011. Protective and pathogenic functions of macrophage subsets. Nat Rev Immunol **11:**723–737. http://dx.doi.org/10.1038/nri3073.
57. **Gupta G, Bhattacharjee S, Bhattacharyya S, Bhattacharya P, Adhikari A, Mukherjee A, Majumdar SB, Majumdar S.** 2009. CXC chemokine-mediated protection against visceral leishmaniasis: involvement of the proinflammatory response. J Infect Dis **200:**1300–1310. http://dx.doi.org/10.1086/605895.
58. **Meier CL, Svensson M, Kaye PM.** 2003. Leishmania-induced inhibition of macrophage antigen presentation analyzed at the single-cell level. J Immunol **171:**6706–6713. http://dx.doi.org/10.4049/jimmunol.171.12.6706.
59. **Murray PJ, Wynn TA.** 2011. Obstacles and opportunities for understanding macrophage polarization. J Leukoc Biol **89:**557–563. http://dx.doi.org/10.1189/jlb.0710409.
60. **O'Garra A, Murphy K.** 1994. Role of cytokines in determining T-lymphocyte function. Curr Opin Immunol **6:**458–466. http://dx.doi.org/10.1016/0952-7915(94)90128-7.
61. **Chakravortty D, Hansen-Wester I, Hensel M.** 2002. Salmonella pathogenicity island 2 mediates protection of intracellular Salmonella from reactive nitrogen intermediates. J Exp Med **195:**1155–1166. http://dx.doi.org/10.1084/jem.20011547.
62. **Miller BH, Fratti RA, Poschet JF, Timmins GS, Master SS, Burgos M, Marletta MA, Deretic V.** 2004. Mycobacteria inhibit nitric oxide synthase recruitment to phagosomes during macrophage infection. Infect Immun **72:**2872–2878. http://dx.doi.org/10.1128/IAI.72.5.2872-2878.2004.
63. **Iniesta V, Carcelen J, Molano I, Peixoto PM, Redondo E, Parra P, Mangas M, Monroy I, Campo ML, Nieto CG, Corraliza I.** 2005. Arginase I induction during Leishmania major infection mediates the development of disease. Infect Immun **73:**6085–6090. http://dx.doi.org/10.1128/IAI.73.9.6085-6090.2005.
64. **Muleme HM, Reguera RM, Berard A, Azinwi R, Jia P, Okwor IB, Beverley S, Uzonna JE.** 2009. Infection with arginase-deficient Leishmania major reveals a parasite number-dependent and cytokine-independent regulation of host cellular arginase activity and disease pathogenesis. J Immunol **183:**8068–8076. http://dx.doi.org/10.4049/jimmunol.0803979.
65. **Adhikari A, Gupta G, Majumder S, Banerjee S, Bhattacharjee S, Bhattacharya P, Kumari S, Haldar S, Majumdar SB, Saha B, Majumdar S.** 2012. Mycobacterium indicus pranii (Mw) re-establishes host protective immune response in Leishmania donovani infected macrophages: critical role of IL-12. PLoS One **7:**e40265. http://dx.doi.org/10.1371/journal.pone.0040265.
66. **Shio MT, Hassani K, Isnard A, Ralph B, Contreras I, Gomez MA, Abu-Dayyeh I, Olivier M.** 2012. Host cell signalling and leishmania mechanisms of evasion. J Trop Med **2012:**819512. http://dx.doi.org/10.1155/2012/819512.
67. **Awasthi A, Mathur R, Khan A, Joshi BN, Jain N, Sawant S, Boppana R, Mitra D, Saha B.** 2003. CD40 signaling is impaired in L. major-infected macrophages and is rescued by a p38MAPK activator establishing a host-protective memory T cell response. J Exp Med **197:**1037–1043. http://dx.doi.org/10.1018/jem.20022033.
68. **Sen E, Chattopadhyay S, Bandopadhyay S, De T, Roy S.** 2001. Macrophage heterogeneity, antigen presentation, and membrane fluidity: implications in visceral leishmaniasis. Scand J Immunol **53:**111–120. http://dx.doi.org/10.1046/j.1365-3083.2001.00856.x.
69. **Rub A, Dey R, Jadhav M, Kamat R, Chakkaramakkil S, Majumdar S, Mukhopadhyaya R, Saha B.** 2009. Cholesterol depletion associated with Leishmania major infection alters macrophage CD40 signalosome composition and effector function. Nat Immunol **10:**273–280. http://dx.doi.org/10.1038/ni.1705.